Malignant Lesions

13

Jacopo Nori, Chiara Bellini, and Claudia Piccolo

13.1 Introduction

Breast cancer is the most common cancer in women, with over 230,000 new cases diagnosed in the United States and 1.5 million new cases of invasive carcinoma diagnosed worldwide each year. For women, there is an approximately 12.4% (1 in 8) individual lifetime chance of developing invasive breast cancer. Breast cancer death rates declined 39% from 1989 to 2015 among women, and this progress was attributed to improvements in early detection [1]. Therefore, the ultimate goal for any breast imaging modality is to decrease the mortality from breast cancer by improving detection at its early stage and diagnosis.

Angiogenesis is the process by which new blood vessels are formed and has been recognized as a key element in the pathophysiology of tumour growth and metastases [2]. Tumours can only grow up to a diameter of 1–2 mm, beyond which neovascularization becomes a necessity, as passive diffusion is no longer sufficient to support the viability of malignant cells [3, 4].

J. Nori (✉) · C. Bellini
Diagnostic Senology Unit, Department of Radiology, Azienda Ospedaliero Universitaria Careggi, Florence, Italy
e-mail: jakopo@tin.it

C. Piccolo
Department of Medicine and Health Science, University of Molise, Campobasso, Italy

Oncologic research has focused on the development of antiangiogenetic and antivascular agents, bringing with it a demand for an accurate means of diagnosing tumour angiogenesis and monitoring treatment responses [5].

At present, magnetic resonance imaging (MRI) is regarded as the gold standard modality to provide functional information on neovascularity as a tumour-specific feature, improving the detection and characterization of breast cancers. MRI demonstrates relatively good spatial resolution and specificity, without ionizing radiation, and has limited side effects [6]. However, despite this increased ability for cancer detection, MRI is limited by its high cost, long acquisition times and low availability.

Contrast-enhanced digital mammography (CEDM) is an emerging breast imaging modality in which contrast enhancement is used with digital mammography to depict tumour neovascularity in a fashion similar to MRI [7–11].

Based on previous literature, CEDM has been demonstrated to be more sensitive than mammography for the detection of breast cancer. It has also shown to have sensitivity comparable to that of MRI at 96–100% for breast cancer detection, with fewer false positive findings in the preoperative setting [12–14]. CEDM is becoming a promising addition to current breast imaging techniques due to its low cost, increasing availability and its ability to be used in women who are contraindicated for MRI [15].

J. Nori, Maninderpal Kaur (eds.), *Contrast-Enhanced Digital Mammography (CEDM)*,
https://doi.org/10.1007/978-3-319-94553-8_13

In this chapter, we aim to review the imaging features of the malignant breast lesions frequently observed during our daily diagnostic work-up and to describe their morphologic and kinetic patterns, with particular mention of CEDM manifestations in our single-institution experience.

13.2 CEDM Malignant Findings

CEDM is an imaging modality which combines digital mammography with intravenous injection of iodinated contrast media to detect hypervascularized lesions. The rationale behind this modality lies in the digital subtraction between two images: one image containing information about breast vascularization and the second about its morphology. Based on the interaction between X-rays and iodine, it is possible to distinguish vascular structures, saturated by contrast agent, by a "high-energy" image (above the k-edge of iodine of 33 keV) and the morphological information by a "low-energy" image (below the 33 keV energy). The subtraction of the two images reveals the "hypervascularized" regions of the mammary gland [16].

CEDM is typically performed as a second-level technique for patients with suspicious focal lesions, when conventional mammography and additional ultrasound (US) examinations fail to make a definitive diagnosis. It is particularly useful in dense breasts or heterogeneously dense breasts (BI-RADS grades C and D), where cancer detection is lowered due to reduced mammographic sensitivity [17].

The hypervascularized appearance of malignant tumours has been emphasized since the first work on contrast-enhanced mammography. Breast cancers are usually characterized by an intense enhancement with spiculated contours in contrast-enhanced digital mammography, as opposed to the rest of the mammary gland, which is little or not at all enhanced. When breast cancer is clinically or radiologically suspected, CEDM may be performed to detect additional homo- or contralateral lesions, enhancing those localizations not spontaneously visible by standard mammograms.

CEDM has been shown to have an excellent correlation with MRI for evaluating the disease extent, although current study results are still based on limited sample sizes [18, 19].

CEDM is also useful in the setting of a second-look examination by ultrasound, helping to identify additional lesions and to more easily decide on those that require a biopsy.

13.3 Malignant Breast Neoplasms

13.3.1 Ductal Carcinoma In Situ (DCIS)

DCIS is a non-invasive malignancy and a non-obligate precursor to invasive cancer. It is characterized by proliferation of malignant ductal epithelial cells lining the terminal ductal-lobular unit, without invasion through the basement membrane, leading to a dilatation of the duct itself [20].

The incidence of DCIS has risen dramatically since the use of screening mammography has strongly increased. According to the literature, multicentricity is observed in 8–33% of cases. In a case series by Lagios et al. [21], they reported that the likelihood of multicentricity increased with tumour size and DCIS lesions measuring over 2.5 cm in diameter were multicentric 47% of the time. Similar results were obtained by Dershaw et al. [22], who observed that all cases of DCIS measuring over 2.5 cm were characterized by multicentric disease and were associated with an increased risk of microinvasive components.

According to these data, it is easy to understand why a correct pre-operative assessment of the disease is mandatory, since it has been demonstrated that patients with positive margins after surgery, as well as patients with residual synchronous foci of DCIS, have increased risk for relapse. The frequency of local recurrence differs

according to the nuclear grade of the lesion, the presence and extent of necrosis or both [23, 24].

The traditional pathologic classification of DCIS is based on the architectural pattern, including cribriform, micropapillary, solid and comedo subtypes. However, this architectural subtype is not prognostic and is independent of the presence of necrosis and the histologic grade. Other classification systems for DCIS have tried to be more reproducible with a significant prognostic impact; among these, the simplest and fittest is the Van Nuys prognostic index system, which divides DCIS into three groups, based on the size, nuclear grade and presence or absence of comedo necrosis. Later, recommendations from the committee of the Consensus Conference on the Classification of DCIS identified three nuclear grades: low, high and intermediate [25, 26].

This digression is essential to better understand the kinetic behaviour of DCIS in CEDM examinations, as explained thereafter.

13.3.1.1 DCIS Findings

– *On mammography*, approximately 80% of DCIS lesions appear as a cluster of calcifications, which may be amorphous, coarse, heterogeneous or fine pleomorphic with a clustered, linear or segmental distribution [27]. The relationship between the histologic grade of DCIS and mammographic calcifications has been a subject of several studies, although only a few have shown a significant correlation; owing to the considerable overlap between the mammographic appearances of the different histologic subtypes, the pathologic grading cannot be determined prospectively with any accuracy on the basis of imaging findings [27]. Fine linear and fine linear branching calcifications seen in a grouped or segmental distribution are usually associated with higher-grade DCIS, whereas amorphous calcifications have been associated with low-grade DCIS. A significant association was found between fine pleomorphic or fine linear branching calcifications and necrosis; furthermore, a significant correlation was encountered between round calcifications and low-grade DCIS.

In 10% of cases, DCIS can also appear as a mass at mammography, possibly related to two different conditions: the opacity could be a direct manifestation of an existing soft-tissue mass or may be a result of periductal fibrosis or elastosis producing an irregular or spiculated margin around a non-mass lesion. Low-grade DCIS appears as masses or asymmetries at imaging, differently from high-grade lesions, which usually manifest as calcified abnormalities. In 7–13% of cases, DCIS may manifest as an architectural distortion [28].

– *On US*, DCIS is infrequently seen, appearing as an intraductal, iso to hypoechoic, microlobulated soft tissue nodule with normal acoustic transmission. Sometimes, suspicious calcifications can be seen, and in those cases, a biopsy could also be performed based on US findings.
– *On MRI*, The sensitivity of MRI for the detection of DCIS has been shown to be higher for high-grade and intermediate-grade DCIS compared with low-grade DCIS (98%, 91% and 80%, respectively) [29, 30]. This observation was also demonstrated by Kuhl et al. [31], where they studied 89 cases of high-grade DCIS, of which 43 (48%) were missed by mammography but diagnosed by MRI alone. In contrast, MRI detected 87 (98%) of these lesions; the two cases missed by MRI were detected by mammography. They concluded that MRI could help improve the ability to diagnose DCIS, especially those with high nuclear grade type. Therefore, MRI is by far more sensitive than mammography in the detection of all grades of DCIS.

DCIS most commonly appears as an area of non-mass enhancement (NME) (60–81%) and less frequently as a mass (14–41%) or as a focus (1–12%) [29, 30].

DCIS may not be visible or hypointense on pre-contrast T1-weighted images and on non-fat-saturated or fat-saturated T2-weighted images because it could be masked by the normal breast parenchyma. DCIS may sometimes appear bright on T2-weighted images because of ductal secretions or necrosis.

In the MRI BIRADS lexicon, NME is defined as an area of enhancement distinct from the surrounding parenchyma, larger than a mass but without space-occupying effect features. The NME area shows stippled or patchy normal glandular tissue or fat within its borders. It is often not detected on pre-contrast images even when correlated with post-contrast images, and follows the distribution of glandular tissue. This imaging entity was unique to MRI until the appearance of CEDM and is usually not detected on mammography and US. The features of NME have been described extensively in Chapter 9 of this book.

Briefly, NME distribution descriptors include symmetric or asymmetric enhancement of the breast tissue. The BIRADS lexicon describes NME distribution as focal, linear, linear branching, segmental, regional, multiple regions and diffuse. NME internal enhancement descriptors are homogeneous, heterogeneous, stippled, clumped or clustered ring enhancement (a recently introduced internal enhancement descriptor).

Stippled enhancement refers to multiple, often innumerable punctuate foci and is usually typical of benign background parenchymal enhancement or fibrocystic changes. Clumped enhancement refers to cobblestone or beaded enhancement, with occasional confluent areas, often suggesting a DCIS in 60–80% of cases [32]. The term "clustered ring enhancement" is a new internal enhancement descriptor, describing "minute ring enhancements", mostly associated with ductal carcinoma in situ and invasive cancers associated with ductal carcinoma in situ. Tozaki and colleagues [33] described this pattern in 63% of malignant lesions, compared with only 4% of benign lesions; a wash-out kinetic pattern was seen in 55% of malignant lesions with clustered ring enhancement. Segmental distribution is the most common pattern of contrast distribution in DCIS (14–77% of cases) [34].

DCIS may appear as an enhancing mass in 14–34% of cases; focal enhancement, the least common finding, is seen in 1–12% of cases. On the other hand, the mixed forms of invasive and DCIS lesions appear as an enhancing mass in 76% of cases [35].

High-grade DCIS more frequently manifests as an enhancing mass than intermediate or low-grade DCIS does. According to Heywang-Köbrunner [36], there is significant variability in DCIS enhancement kinetics, with some lesions showing delayed enhancement. Furthermore, several studies have demonstrated that the qualitative enhancement patterns differ significantly according to lesion type. Mass lesions more often exhibit rapid uptake of contrast medium in the initial phase and rapid wash-out compared with non-mass lesions.

– *On CEDM*, detecting and staging DCIS is still under debate: similar to MRI, CEDM is capable of detecting non-calcified DCIS, providing a better tumour size assessment, in comparison with full-field digital mammography (FFDM). Unlike MRI, CEDM can also spot calcifications, which are seen as "negative contrast enhancement" artefacts, thus improving the diagnostic performance.

A recent study by Cheung et al. [37] focused on screening patients referred for CEDM to evaluate the presence of enhancement of areas of suspicious calcifications. They found that enhancement of areas with calcifications on CEDM significantly improved the cancer prediction rate, with a PPV of 46.15% for amorphous and 90% for pleomorphic calcifications and that all these types of findings were characterized by a high NPV of approximately 95%. The authors concluded that the enhancement detected in CEDM could be considered an adjuvant tool for assessing the study of calcifications. Another study by Luczynska et al. [38],

which compared the degree of enhancement on CEDM with mammographic findings and histopathological results, reported that 87.5% of DCIS lesions (presenting as calcifications or a mass with associated calcifications on FFDM) showed weak enhancement, with no false-negative cases.

– In our preliminary experience with 157 malignant lesions detected on CEDM, DCIS accounted for 13%, and DCIS associated with invasive elements accounted for 6%; there was no dominant pattern of presentation observed, with mass, NME and ring enhancement all manifesting with the same frequency for pure DCIS, while the pattern associated with invasive ductal carcinoma (IDC) presented itself in 42% of cases as a mass, in 42% of cases as NME and in 16% of cases as ring enhancement.

The kinetics of enhancement was characterized by a delayed enhancement in the majority of cases. A possible explanation for this finding may rely on the relative lack of blood supply and the diffusibility of contrast media to the ducts. As addressed by Fallenberg et al. [39], the possible explanation for this would be that the amount of contrast reaching the tissue by diffusion is time dependent. Therefore, longer time delays between contrast injection and CEDM exposure can result in stronger enhancement and better visibility of DCIS (Figs. 13.1 and 13.2).

For DCIS associated with IDC, 58% of lesions showed a progressive enhancement, and 42% exhibited a prompt wash-out.

13.3.2 Invasive Ductal Carcinoma, Not Otherwise Specified (IDC NOS)

Invasive ductal carcinoma accounts for 65–80% of breast cancers [40–42].

IDC is the most common invasive malignant breast tumour. At gross analysis, it appears as a solid mass, with various degrees of necrosis and haemorrhage.

The morphologic patterns can have a wide variation, depending on its clinical and biological features.

13.3.2.1 IDC Findings

– *On mammography*, IDC usually appears as a scirrhous, radiodense and irregular mass, often associated with a stromal desmoplastic reaction, responsible for spiculated margins; when calcifications manifest, they generally suggest an associated intraductal component. Less frequently, invasive ductal carcinomas are well defined, with a lobulated shape and circumscribed margins.
– *On US*, the typical finding is an inhomogeneous and hypoechoic lesion with irregular margins surrounded by a hyperechoic rim with posterior shadowing and increased vascularity on colour Doppler analysis.
– *On MRI*, owing to its high cellularity, IDC appears as a hypointense lesion on T2-weighted images. However, some of them may manifest as a high signal intensity on T2-weighted images because of the presence of necrosis, a finding suggesting a poorly differentiated high-grade carcinoma; extensive necrosis within an invasive breast carcinoma may be indicative of a rapid growth rate and an unfavourable prognosis [36, 41].

The majority of IDCs follow the “90/90 rule”: they enhance by 90% within the first 90 seconds after contrast medium injection.

The kinetics of IDC is typical of a malignant lesion, characterized by early enhancement with rapid uptake of contrast medium followed by wash-out (type III) in half of the cases and by a plateau in 40% of cases (type II). Just a few (5%) manifest a type I curve with a mild and progressive enhancement, a pattern reflecting a low-density lesion with abundant fibrosis, as occurs in the scirrhous type [36].

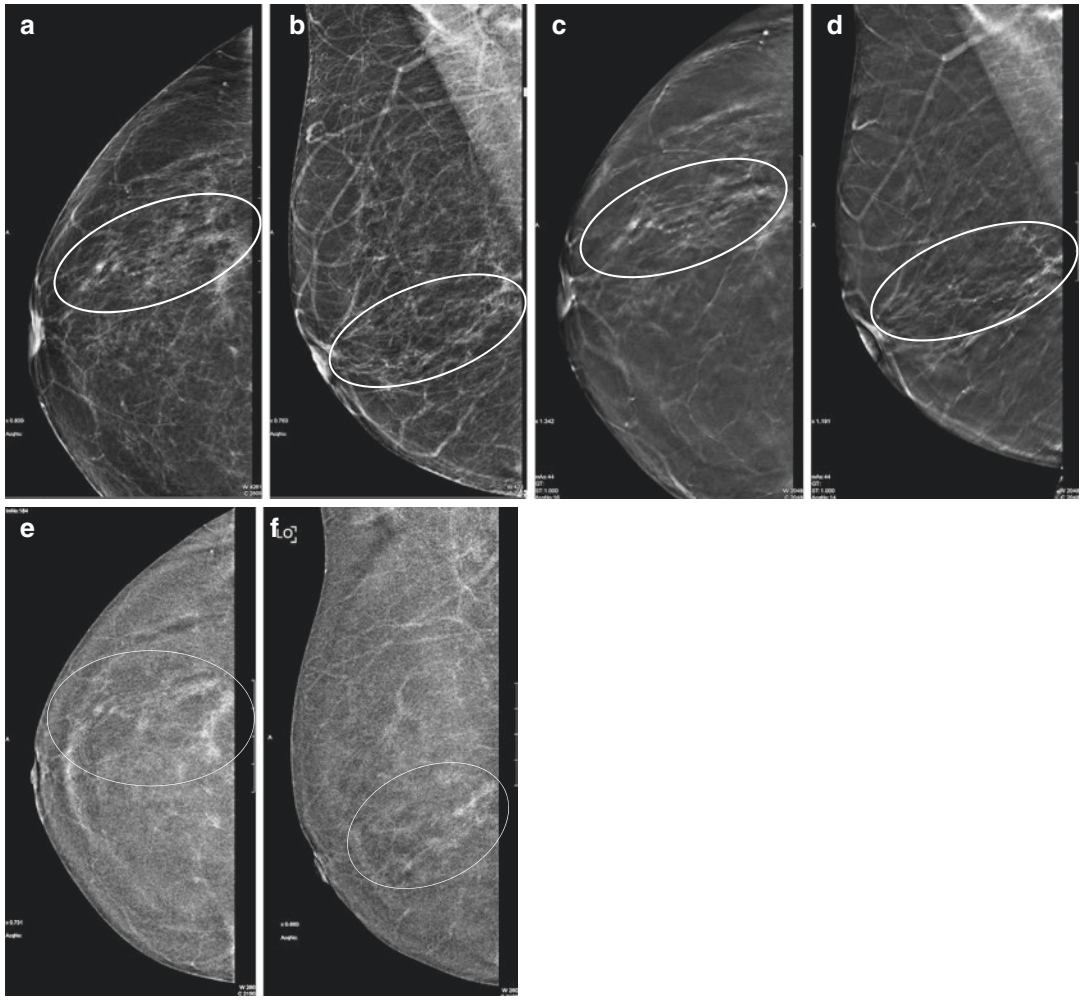

Fig. 13.1 Pre-surgical staging in a patient with a BI-RADS 5 lesion in the mid-outer quadrant of the right breast, already biopsied. (**a**, **b**) Low energy 2D images in CC and MLO projections show a cluster of fine pleomorphic calcifications in a linear pattern of distribution (*circles*). (**c**, **d**) 3D in CC and MLO projection demonstrates a linear pattern of architectural distortion along the segmental distribution of the calcifications (*circles*). (**e**, **f**) CEDM recombined image in CC and MLO projection. The examination demonstrates a faint non-mass enhancement in the lower-outer quadrant of the right breast, tracking along the distribution of the calcifications. *Diagnosis: The pathology was a ductal carcinoma in situ (DCIS)*

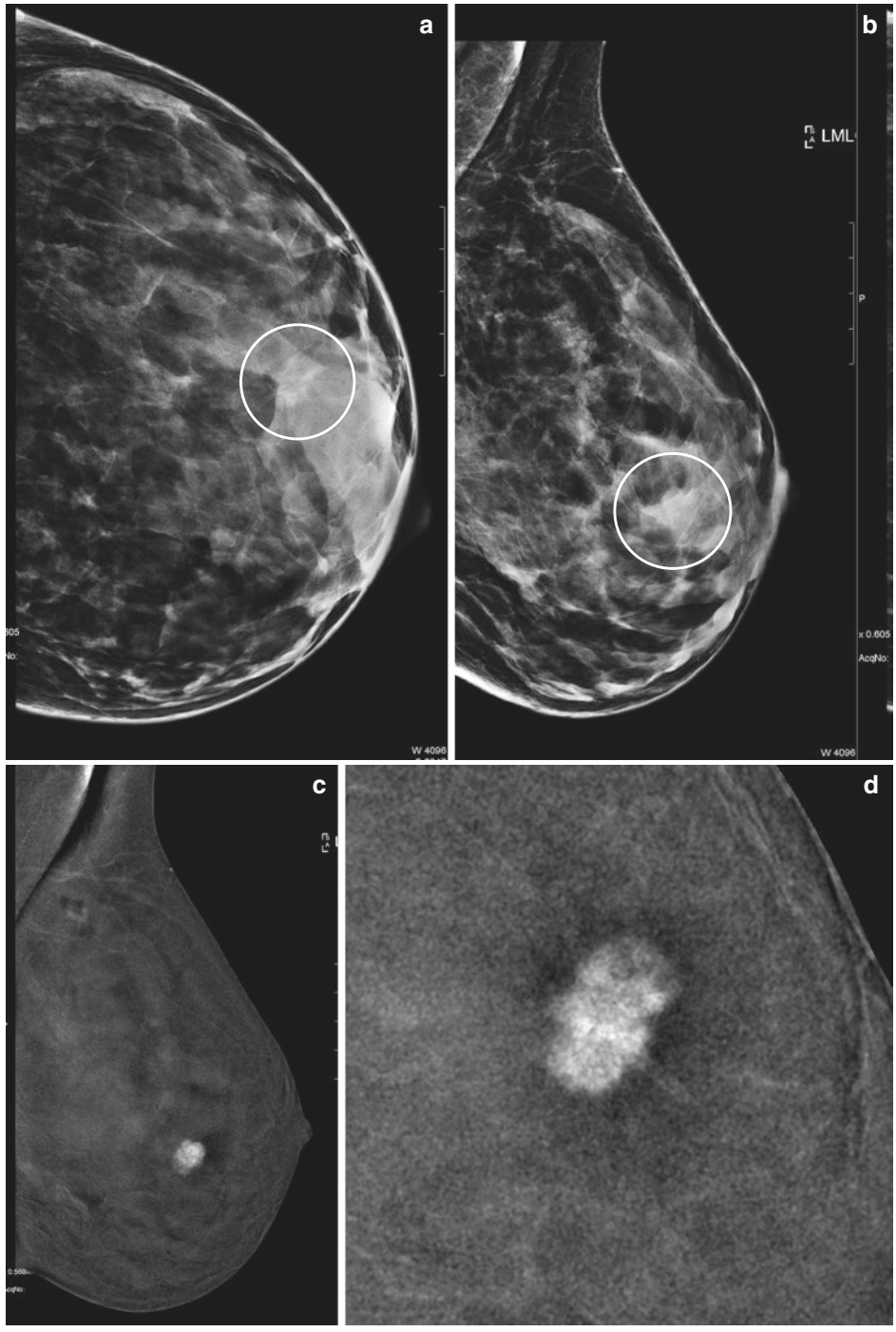

Fig. 13.2 Pre-surgical staging in a patient with a BI-RADS 5 lesion in the central-outer quadrant of the left breast. (**a**, **b**) Low energy 2D images in CC and MLO projections demonstrate a dense breast with reduced diagnostic capability. However, there appears to be a lobulated mass with spiculated margins and associated architectural distortion (*circles*) at the lower outer quadrant. (**c**, **d**) CEDM recombined image in CC projection and magnification view of the lesion. The examination shows an intensely enhancing malignant lesion with irregular borders, better depicted on the magnified view. *Diagnosis: The pathology was an invasive ductal carcinoma*

– *On CEDM*, invasive ductal carcinoma may present as a mass characterized by a prompt intense enhancement with irregular and/or spiculated margins [26]. Less frequently, IDC can present as a round, regular mass or as a NME. It often shows an early wash-out and thus is less enhanced in the delayed images. Small foci of enhancement, near the index lesion, should be considered suspicious for satellite lesions in the differential diagnosis of multicentric/multifocal disease. If there are any new enhancing lesions identified, we usually perform a second-look US and also a second-look review of the tomosynthesis images. This will be followed by either an US or tomosynthesis guided biopsy if they are visible. In addition, the association with a NME or a linear enhancement ("comet tail sign") may be suggestive of an associated in situ component. Comparison with the contralateral breast helps to differentiate between a new lesion and normal bilateral parenchymal background enhancement (BPE), especially in cases with a severe BPE.
– In our experience, ductal invasive carcinoma accounted for 50% of invasive carcinomas. CEDM detected 71 tumours out of 74, with a specificity of 96% and three false negative results, due to severe background parenchymal enhancement. IDC appeared as a mass with spiculated and irregular margins in 96% of cases and as NME in 4% of cases and displayed no ring enhancement. The IDC kinetics reflects that of a highly vascularized lesion with anarchic vessels, showing prompt wash-out in 69% of cases, progressive enhancement in 27% of cases and the absence of enhancement in the remaining 4% of cases (Figs. 13.3, 13.4, 13.5, 13.6, 13.7, 13.8, 13.9, and 13.10).

13.3.3 Subtypes of Invasive Ductal Carcinoma

13.3.3.1 Mucinous Carcinoma

Mucinous carcinomas, known also as colloid carcinomas, account for 1–7% of all breast cancers and have a better 5- to 10-year survival than the usual infiltrating duct carcinoma. Histologically, mucinous carcinoma is characterized by "large amounts of extracellular epithelial mucus, sufficient to be visible grossly, and recognizable microscopically surrounding and within tumour cells" [42].

Two subtypes of mucinous carcinoma may be differentiated histologically: pure and mixed. Of these two subtypes, pure mucinous carcinoma is characterized by less aggressive growth and less frequently metastasizes to axillary lymph nodes [42].

Mucinous Carcinoma Findings

– *On mammography*, mucinous carcinoma usually appears as a round and well-defined mass with regular borders without calcifications.
– *On US*, mucinous carcinoma often displays mixed echogenicity with solid and cystic components. Posterior acoustic enhancement is common. At times the lesion can be isoechoic to breast tissue on ultrasound which can make diagnosis difficult. Due to its high intralesional mucinous component, it may not demonstrate increased vascularity on colour Doppler analysis. All these findings may make it difficult to differentiate mucinous carcinoma from inflamed cysts or benign lesions.
– *On MRI*, mucinous carcinoma appears as a homogeneous and lobular mass. They are one of the few cancers that are markedly hyperintense on T2-weighted images, which relates to the water component in mucin, and they demonstrate a persistent enhancement pattern on dynamic MRI images (including a rim-like peripheral or heterogeneous internal enhancement). Thus, mucinous carcinoma has MRI features of both benignity and malignancy (i.e. rim-like or heterogeneous enhancement). The combination of these MRI findings is useful for accurate diagnosis of the tumour [43, 44].
– *On CEDM*, in our personal series, mucinous tumours, which accounted for 4% of all cancers at our centre, manifested as a mass in all the cases. The kinetics was typical for a malig-

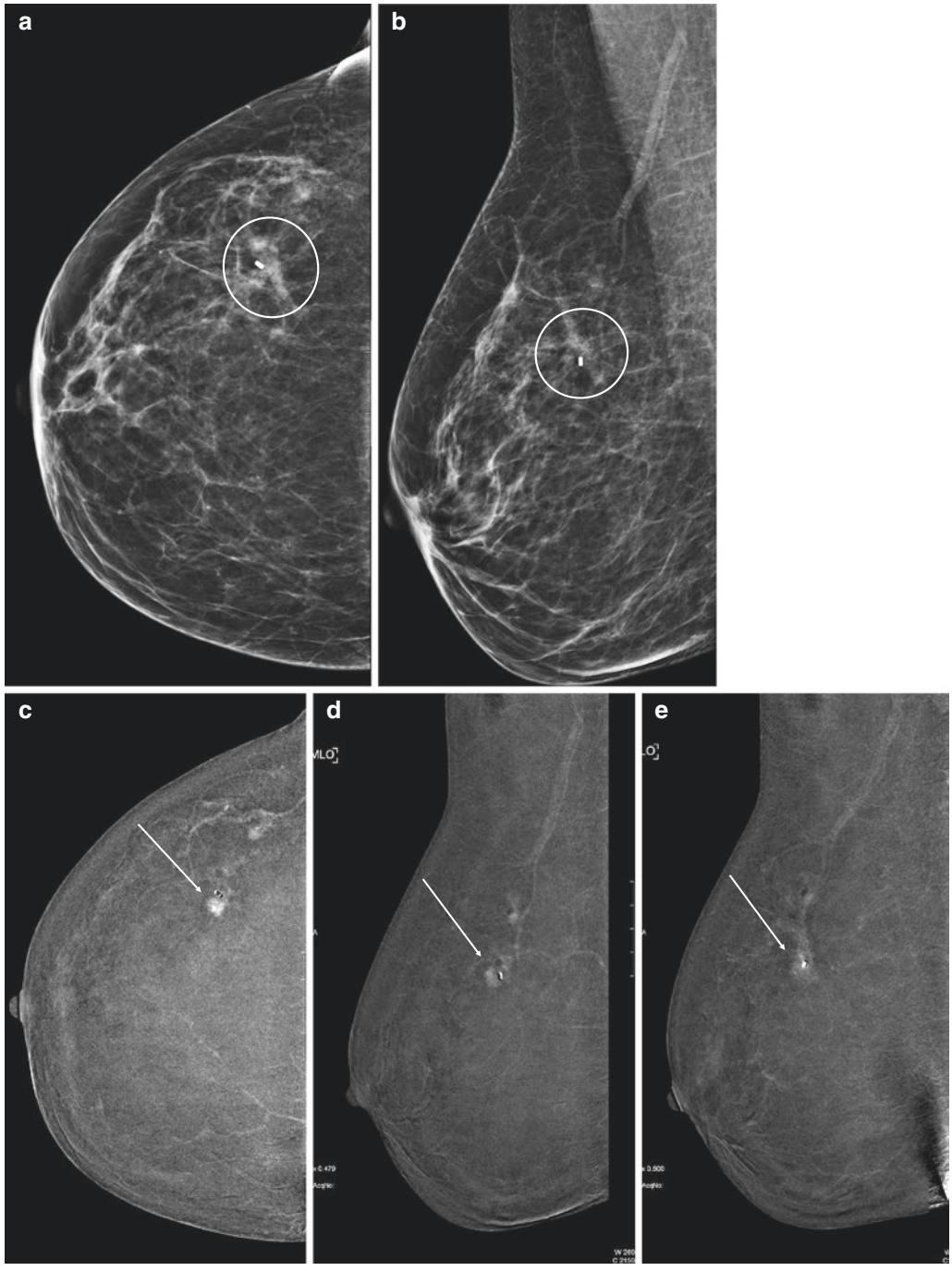

Fig. 13.3 Pre-surgical staging in a patient with a BI-RADS 6 lesion in the upper-outer quadrant of the right breast. (**a**, **b**) Low energy 2D images in CC and MLO projections show a subcentimeter opacity with spiculated margins in the right upper-outer quadrant associated with a small cluster of calcifications and a post vacuum assisted biopsy (VAB) marker in situ (*circle*). (**c**) CEDM recombined image in CC projection. (**d**, **e**) CEDM recombined image in the early and late phase in MLO projection. The examination demonstrates an intensely enhancing mass together with a non-mass linear enhancement, tracking along the distribution of the calcifications. The lesion is better delineated in the delayed MLO phase. *Diagnosis: The pathology was an invasive ductal carcinoma associated with a ductal carcinoma in situ component*

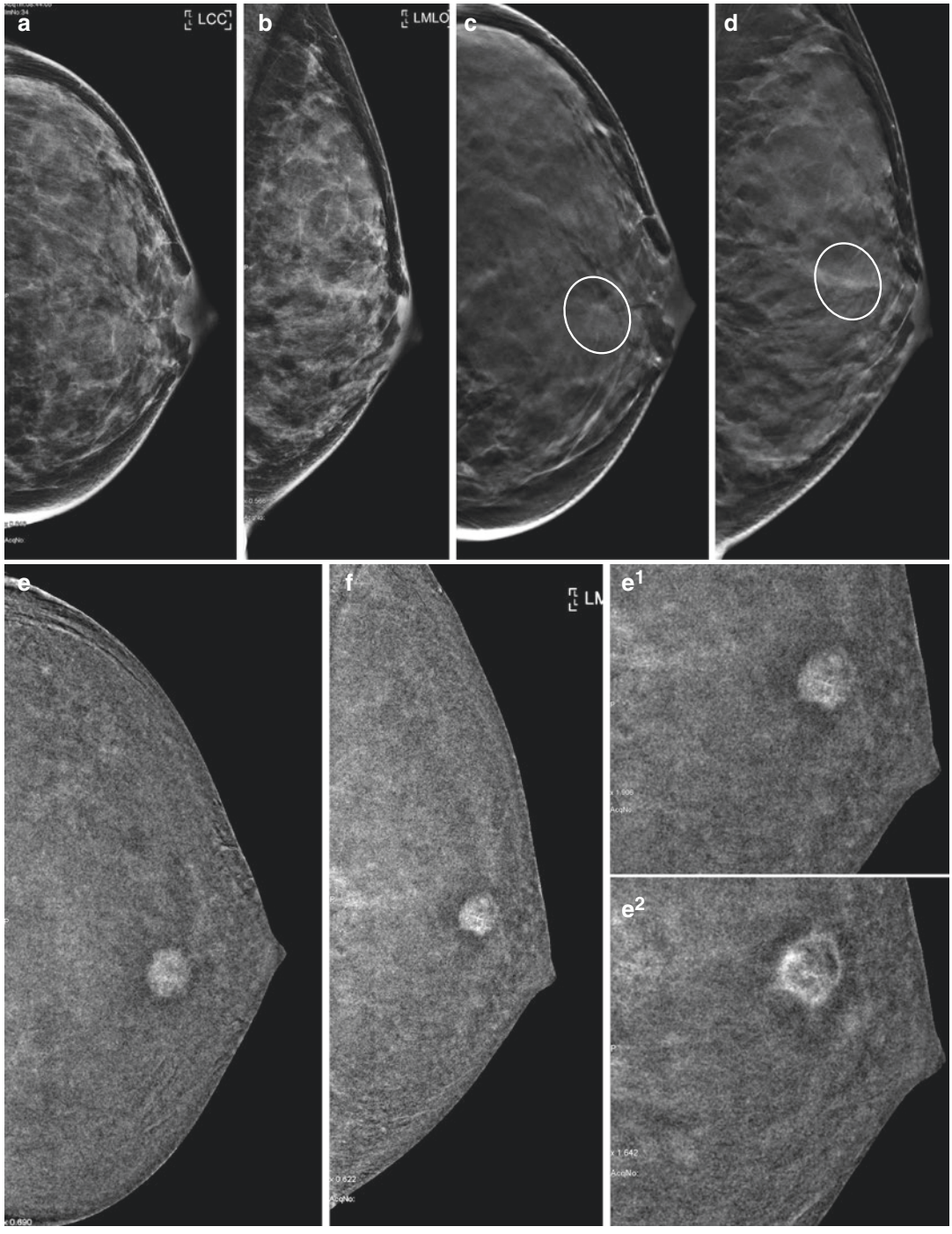

Fig. 13.4 Pre-surgical staging in a patient with a BI-RADS 6 lesion in the upper-outer quadrant of the left breast. (**a**, **b**) Low energy 2D images in CC and MLO projections demonstrated dense breast parenchyma with no significant abnormality. (**c**, **d**) 3D in CC and MLO projection demonstrates a suspicious opacity and architectural distortion in the retro-areolar region (*circle*). (**e**, **f**) CEDM recombined image in CC and MLO projection. (**e**^{1}, **e**^{2}) Magnification views of the lesion in early and late phases. The examination shows a suspicious intensely enhancing mass with no significant wash-out seen in delayed images (*magnification views*). *Diagnosis: The pathology was an invasive ductal carcinoma*

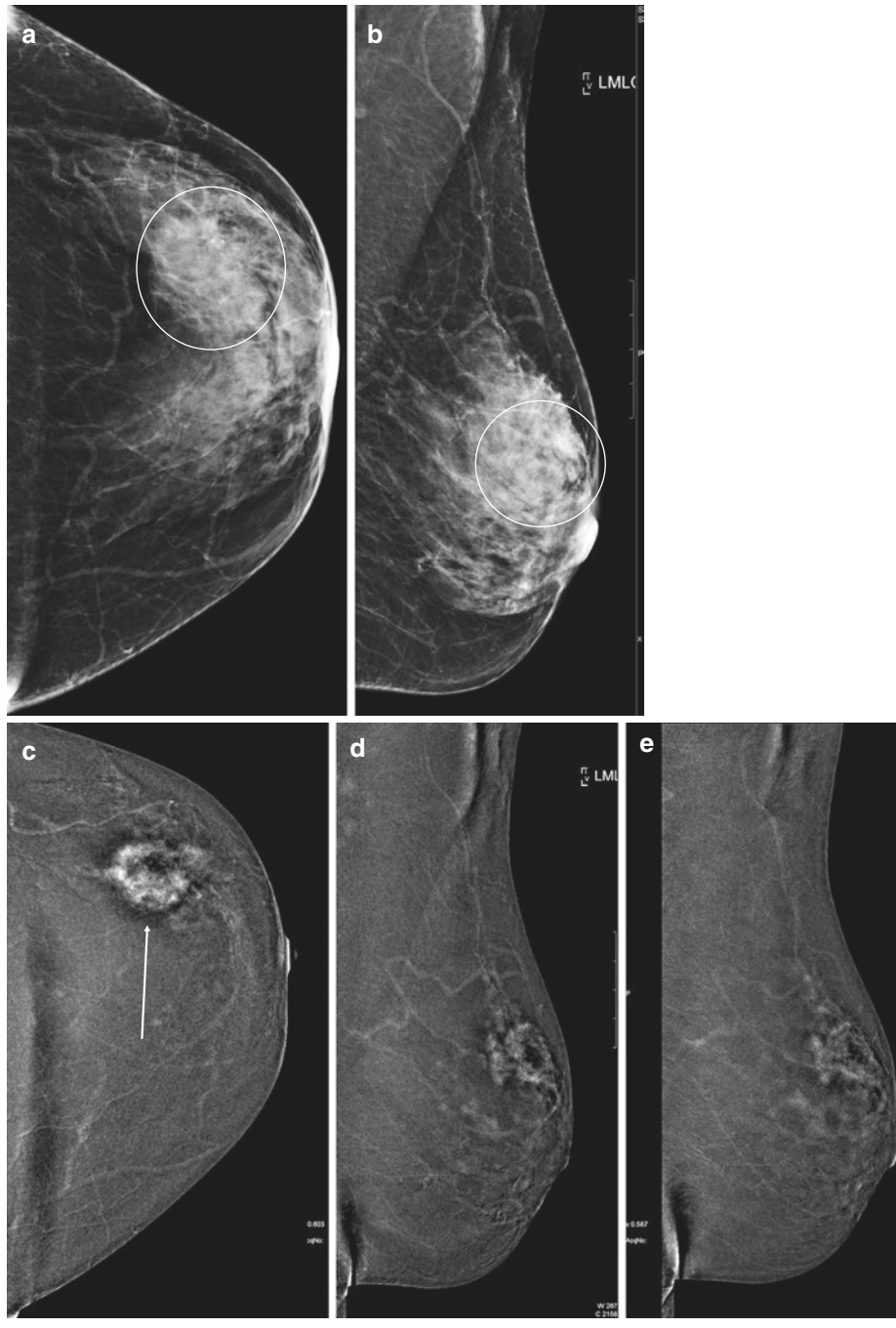

Fig. 13.5 Pre-surgical staging in a patient with a palpable mass in the upper-outer quadrant of the left breast. (**a**, **b**) Low energy 2D images in CC and MLO projections show a dense breast, with an asymmetrical area of increased density (with respect to the other side, not shown) particularly in the left upper-outer quadrant. (**c**) CEDM recombined image in CC projection. (**d**, **e**) CEDM recombined image in the early and late phase in MLO projection. The examination reveals an enhancing mass with irregular borders and a non-enhancing necrotic core (*arrow*) with wash-out in the delayed phase. *Diagnosis: The pathology was an invasive ductal carcinoma*

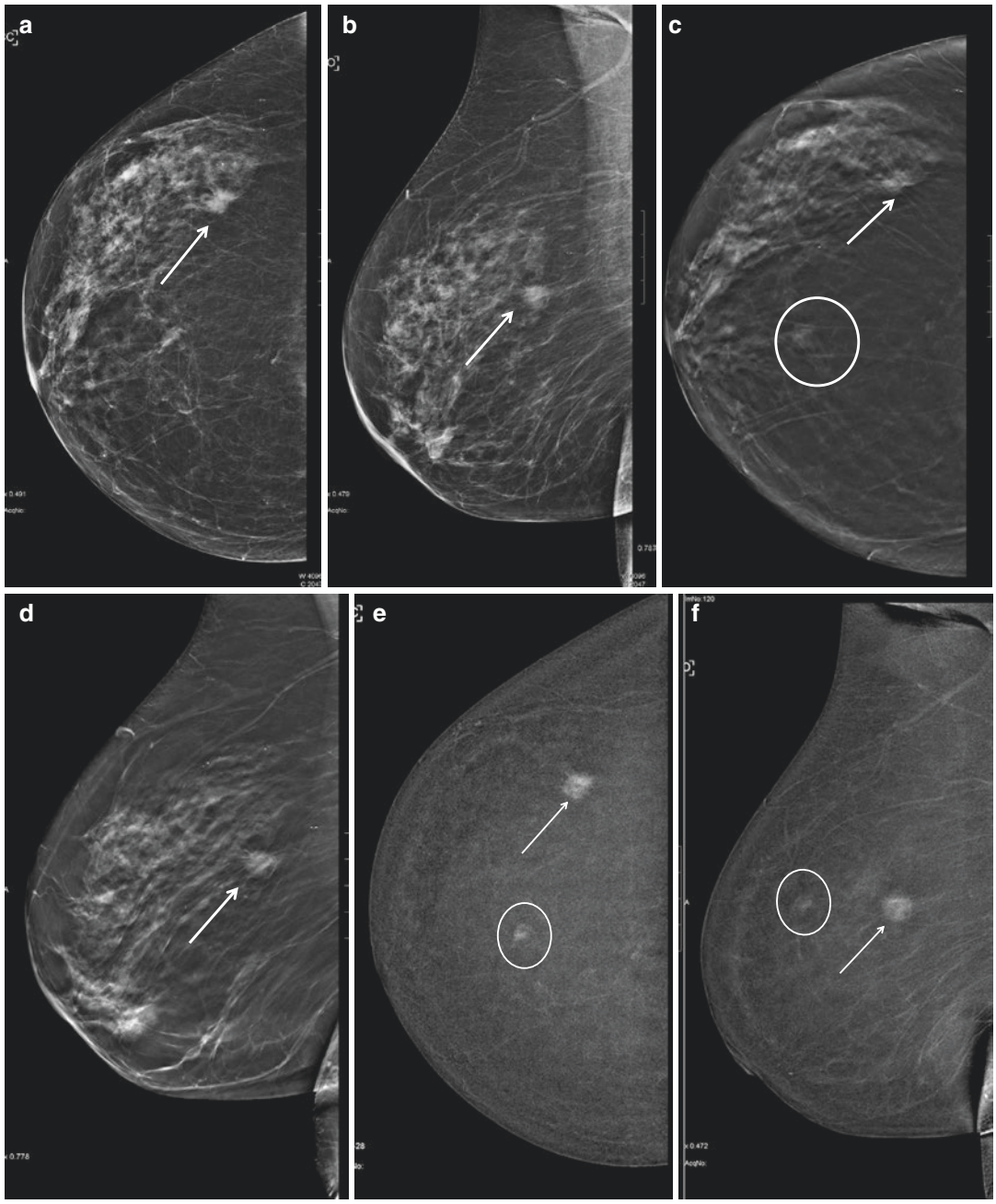

Fig. 13.6 Pre-surgical staging in a patient with a BI-RADS 6 lesion in the central-outer quadrant of the right breast. (**a**, **b**) Low energy 2D images in CC and MLO projections show a highly suspicious mass with irregular borders in the central-outer quadrant (*arrows*). (**c**, **d**) 3D in CC and MLO projections better depicts the features of the suspected mass, and it also demonstrates another new smaller lesion anterior to it (*circle*). (**e**, **f**) CEDM recombined image in CC and MLO projection. The examination shows an intensely enhancing malignant lesion (*arrow*) with irregular borders in the upper outer quadrant, and the other smaller lesion (*circle*) seen on 3D also demonstrated a similar enhancement pattern. *Diagnosis: The pathology of both lesions was invasive ductal carcinoma*

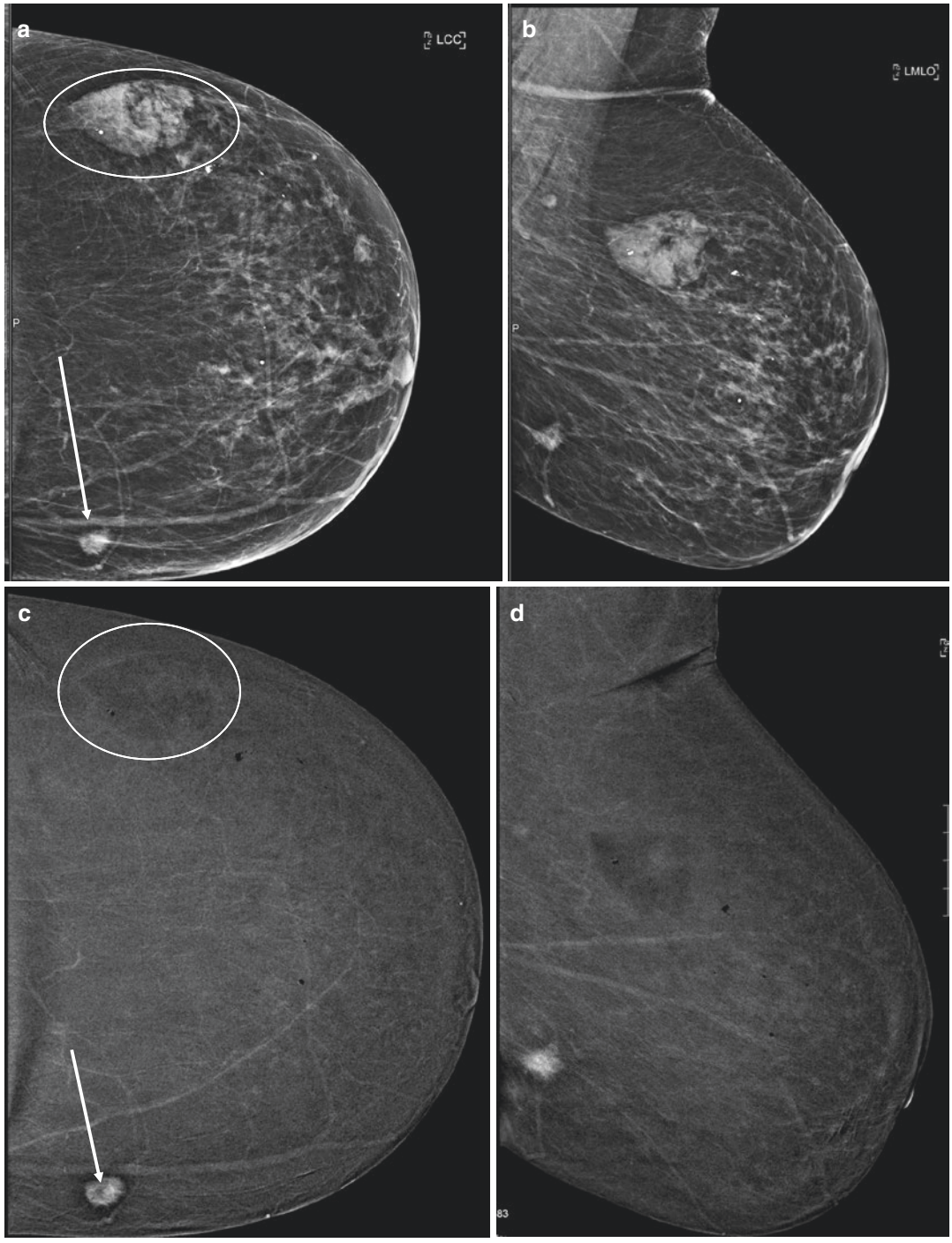

Fig. 13.7 Pre-surgical staging in a patient with a BI-RADS 6 lesion in the lower-inner quadrant of the left breast (*arrow*). (**a**, **b**) Low energy 2D images in CC and MLO projections show a deep-seated suspicious opacity in the lower inner quadrant. There is also a large opacity with lobulated borders seen in the upper outer quadrant (*circle*). (**c**, **d**) CEDM recombined images in CC and MLO projection. The examination shows an intensely enhancing malignant lesion, with irregular borders (*arrow*). The lesion in the upper-outer quadrant showed no enhancement. *Diagnosis: The pathology was an invasive ductal carcinoma (arrow) and a fat lobule (circle)*

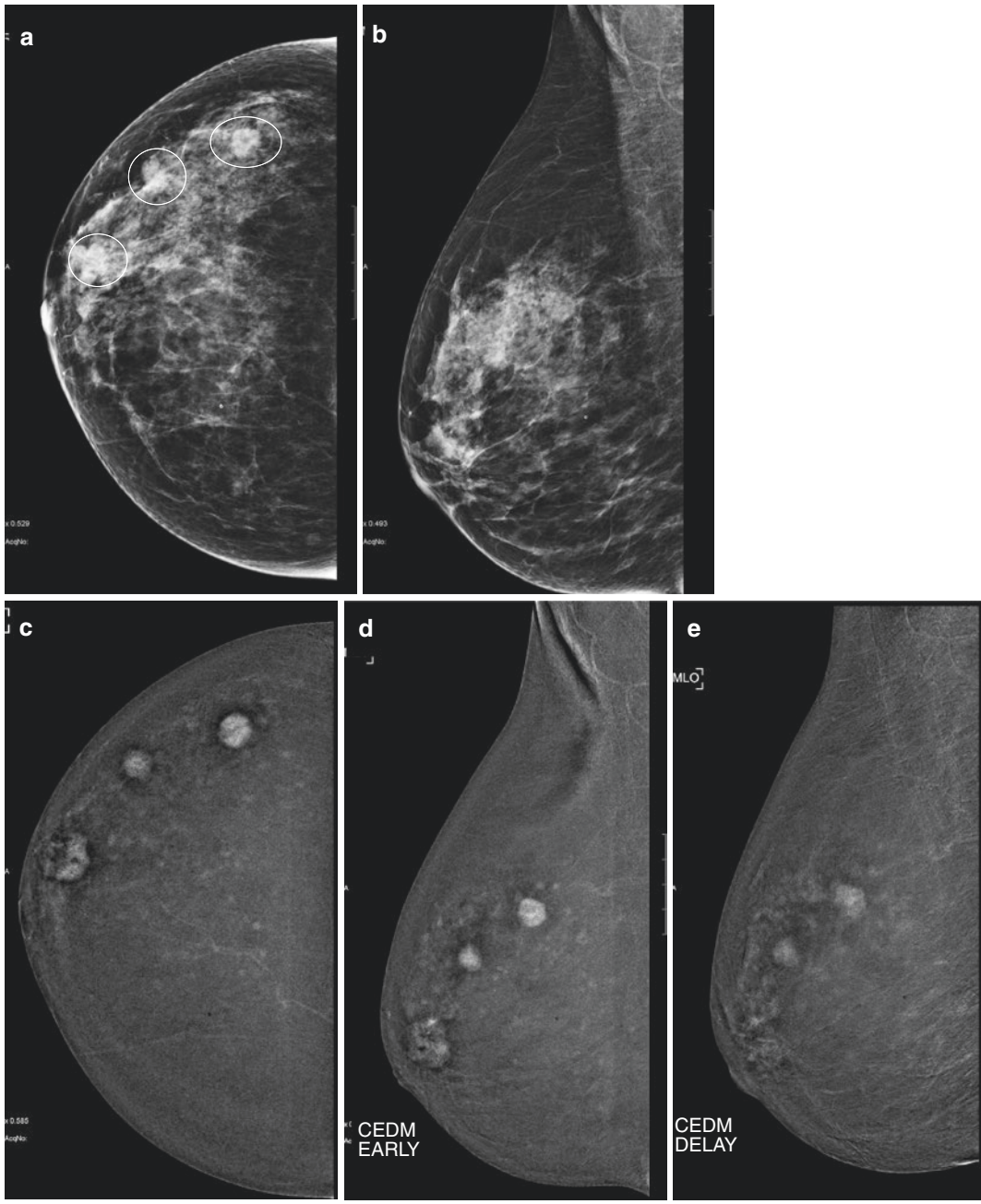

Fig. 13.8 Further evaluation of a patient with a palpable mass in the retro-areolar area of the right breast. (**a**, **b**) Low energy 2D images in CC and MLO projections show an area of increased density in the retro-areolar region, with at least two other masses further away in the outer quadrant. (**c**) CEDM recombined image in CC projection. (**d**, **e**) CEDM recombined image in the early and late phase in MLO projection. The examination shows the known lesion in the retroareolar region that demonstrates enhancement in the early phase with wash-out in the late phase; it also depicts two other lesions with the similar kinetics of enhancement, indicating multifocality. *Diagnosis: The pathology was colloid tumour*

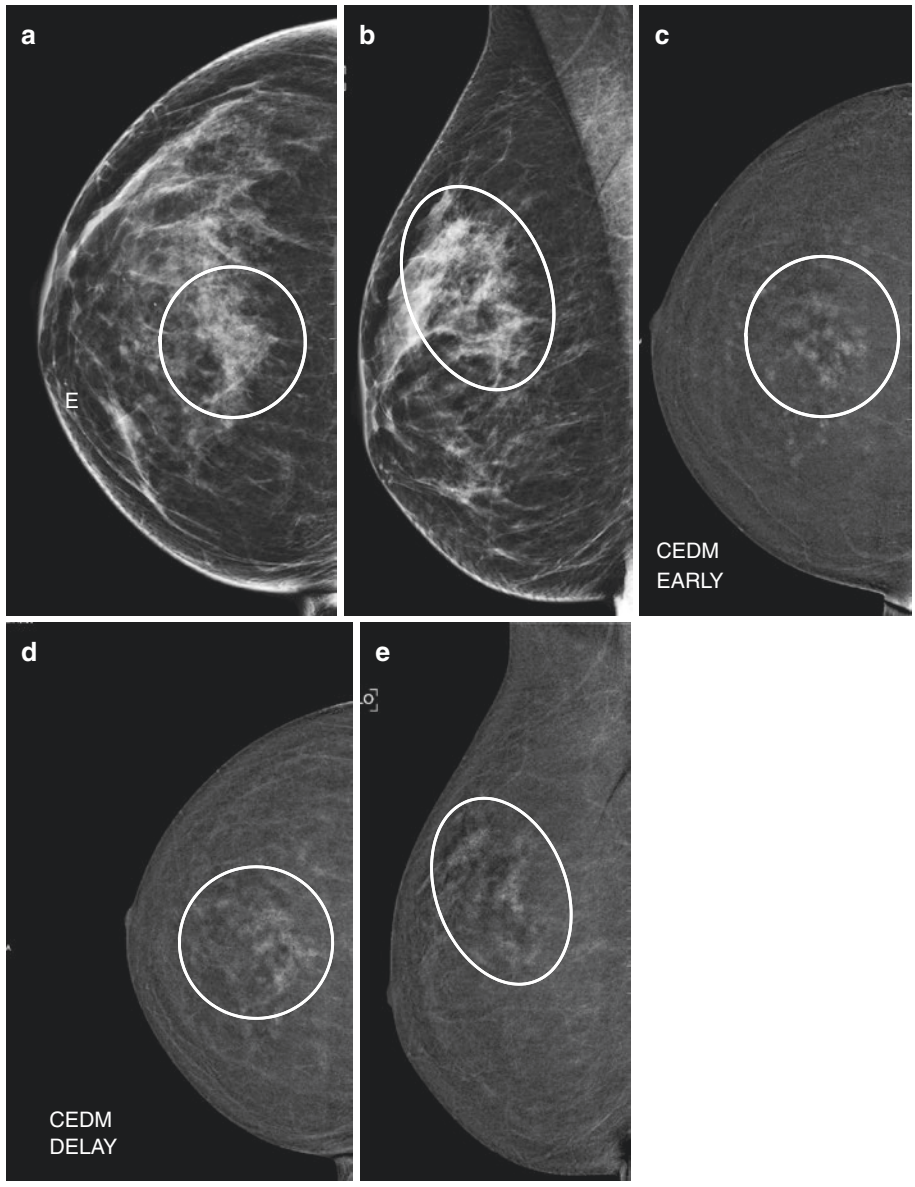

Fig. 13.9 Pre-surgical staging in a patient with a BI-RADS 6 lesion in the central-upper quadrant of the right breast. (**a**, **b**) Low energy 2D images in CC and MLO projections show an asymmetrical area of increased density (*with respect to the other side, not shown*) in the central upper quadrant. (**c**, **d**) CEDM recombined image in the early and late phase in CC projection. (**e**) CEDM recombined image in MLO projection. The examination shows the known lesion presenting as a non-mass enhancement with a clustered distribution demonstrating progressive enhancement on the recombined CC views (*circles*). Owing to the discordance between the mammogram, US (*not shown*), and CEDM findings, the patient underwent a MR examination. (**a'**–**e'**) Subtracted images of the dynamic T1-weighted sequence on axial plane. MR also demonstrated progressive enhancement kinetics, as observed on CEDM examination. In the upper-central quadrant of the right breast one can observe the lesions (*circles*) associated with a clustered non-mass enhancement also extending to the upper-inner quadrant. (**e'**) STIR T2-weighted image on axial plane depicts an asymmetric glandular distortion, with respect to the other side (*not shown*). (**f'**) MIP reconstruction demonstrates the angiogenic vessels (*arrows*) associated with the index lesion. *Diagnosis: The pathology was a colloid tumour*

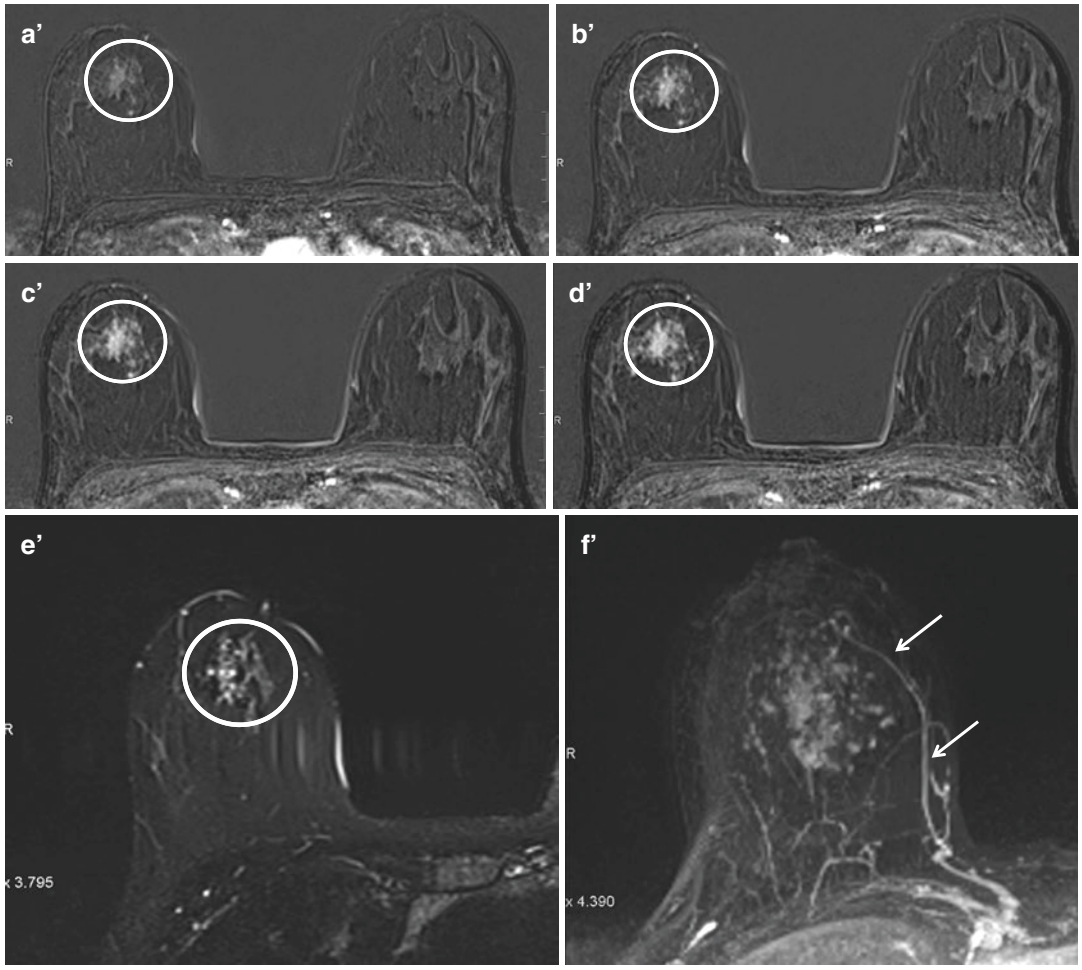

Fig. 13.9 (continued)

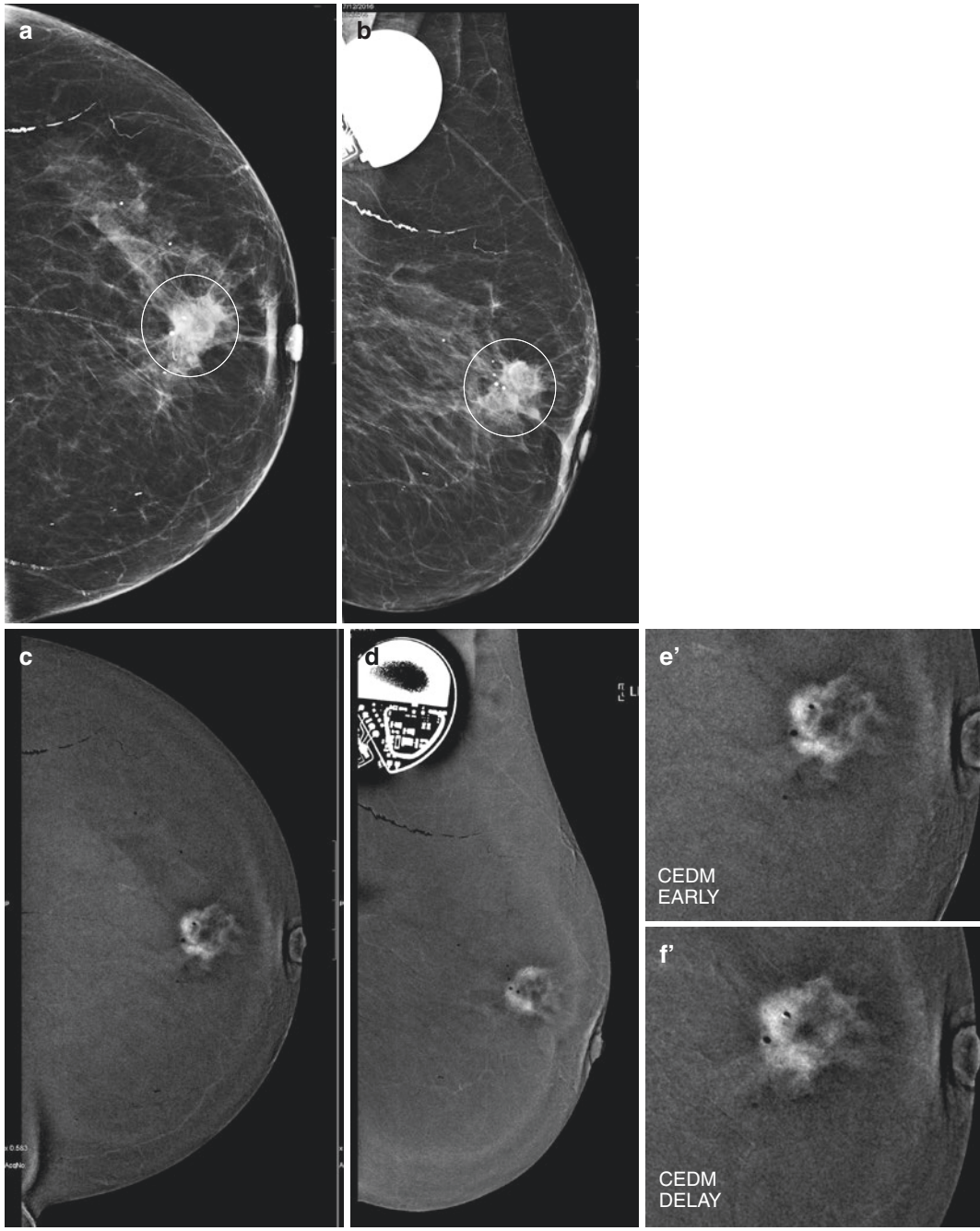

Fig. 13.10 Pre-surgical staging in a patient with a BI-RADS 6 non-palpable lesion in the central-outer quadrant of the left breast. (**a**, **b**) Low energy 2D images in CC and MLO projections show a highly suspicious mass with irregular borders in the central-outer quadrant. (**c**, **d**) CEDM recombined image in CC and MLO projections. (**e**, **f**) Magnification views of the lesion in the early and late phase. The examination shows an intensely enhancing mass demonstrating an early enhancement with no wash-out, as demonstrated by the comparison between the two phases, in the magnification views. The presence of a cardiac pacemaker device was a contraindication for the patient to undergo a MR examination. *Diagnosis: The pathology was a colloid infiltrative carcinoma*

nant lesion, with wash-out in 72% of cases; in 14% of cases, we observed an early and rapid uptake of contrast medium with a subsequent plateau phase, and in the remaining 14% of cases, we observed a gradual and steady persistent enhancement (Figs. 13.11, 13.12, and 13.13).

13.3.3.2 Papillary Carcinoma

Papillary carcinoma is a rare tumour, accounting for 1–2% of breast cancers [45]. The histologic hallmark of all papillary tumours, whether benign or malignant, is arborization of the fibrovascular stroma supporting the epithelial component. The cytomorphology is distinctive, with the presence of single papillae and papillary clusters. An absent myoepithelial layer distinguishes papillary carcinomas from benign papillary lesions.

The tumour is described as an intracystic papillary carcinoma in the presence of a cystic component.

Papillary Carcinoma Findings

- *On mammography*, the features of papillary carcinoma resemble those of medullary carcinoma, with more peripherally located calcifications and a higher density.
- *On US*, papillary carcinoma usually appears as a hypoechoic and solid mass, often with posterior acoustic enhancement; alternatively, they may present as complex cyst with solid components within.
- *On MRI*, the characteristics have been described as an intensely enhancing mass with irregular or rounded borders and non-enhancing internal septae. It is typically heterogeneous, with multiple nodular masses of intermediate signal intensity pro-

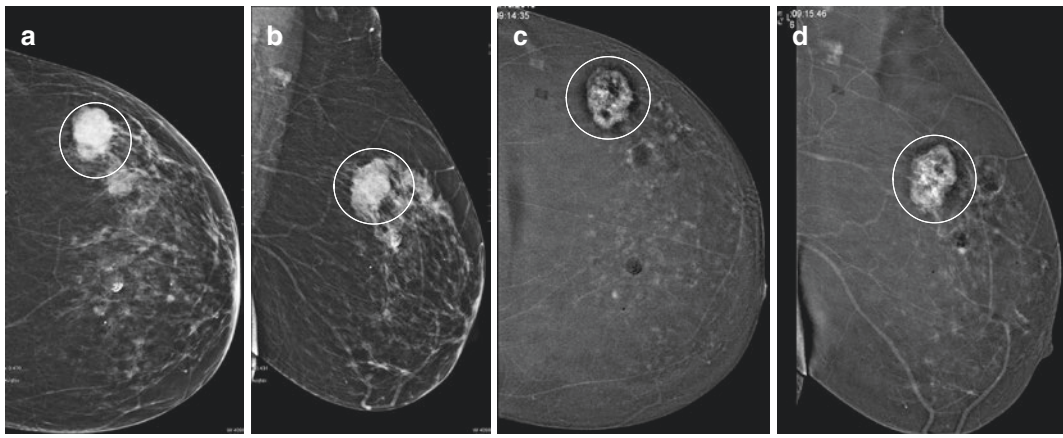

Fig. 13.11 Pre-surgical staging in a patient with a BI-RADS 6 palpable lesion in the upper-outer quadrant of the left breast. (**a**, **b**) Low energy 2D images in CC and MLO projections show a suspicious mass with spiculated borders in the upper-outer quadrant. (**c**, **d**) CEDM recombined image in CC and MLO projection demonstrates an intensely enhancing mass with irregular borders, associated with non-enhancing necrotic areas within it. *Diagnosis: The pathology was a papillary carcinoma*

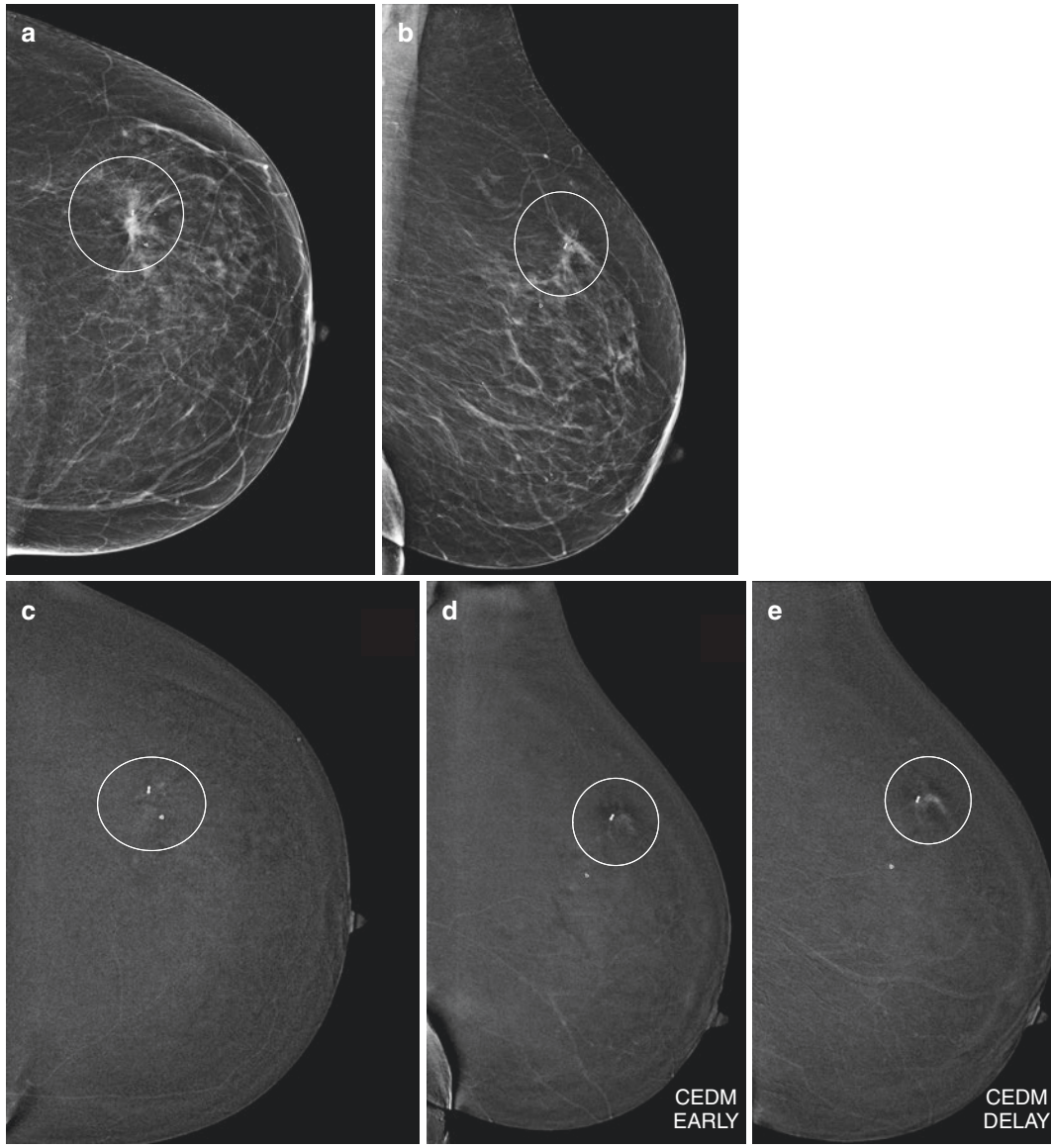

Fig. 13.12 Pre-surgical staging in a patient with a BI-RADS 6 lesion in the upper-outer quadrant of the left breast. (**a**, **b**) Low energy 2D images in CC and MLO projections show an area of architectural distortion in the upper-outer quadrant with post biopsy markers in situ. (**c**, **d**) CEDM recombined image examination in CC and MLO projections demonstrates a small area of non-mass enhancement with persistent to progressive enhancement kinetics as seen on the MLO early and delayed phase. *Diagnosis: The pathology was a tubular carcinoma*

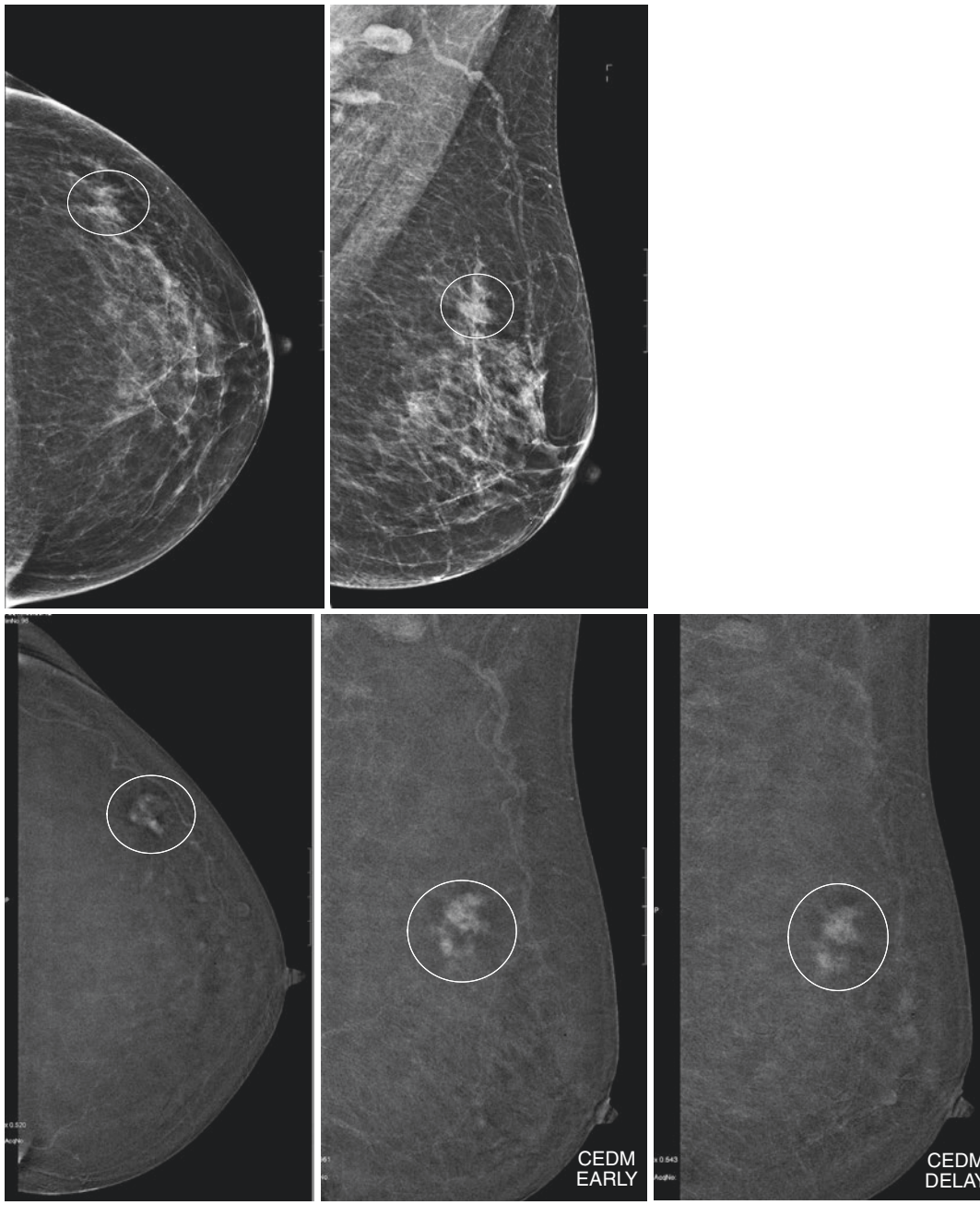

Fig. 13.13 Pre-surgical staging in a patient with a BI-RADS 6 non-palpable lesion in the upper-outer quadrant of the left breast. (**a**, **b**) Low energy 2D images in CC and MLO projections show a suspicious mass with spiculated borders in the upper-outer quadrant. (**c**) CEDM recombined image in CC projection. (**d**, **e**) CEDM recombined image in the early and late phase in MLO projection. The examination shows an intensely enhancing mass with spiculated borders, which is seen to demonstrate a subtle wash-out in the late phase. *Diagnosis: The pathology was a tubular carcinoma*

jecting from the periphery into the lumen [46, 47].

The signal intensity is also dependent on the intracystic fluid composition:

- If serous, it will be hypointese on T1-weighted images and hyperintense on T2-weighted images.
- If there are haemorrhagic contents, it will be hyperintense on both T1- and T2-weighted images, and fluid-fluid levels may be seen on T2-weighted images.
  - *On CEDM*, papillary cancer accounted for 4% of all malignant lesions in our personal series. The morphologic pattern of presentation was a mass in 63% of cases, NME in 25% of cases and rim enhancement in the remaining 12% of cases. The kinetics pattern was characterized by a progressive enhancement in 62% of cases and as an early wash-out in 38% of cases (Fig. 13.14).

13.3.3.3 Tubular Carcinoma

Tubular carcinoma accounts for less than 2% of all breast cancers and for approximately 20% of cancers detected by mammography. It usually affects women in their mid-to-late 40s, slightly younger than for breast cancer in general. At gross examination, tubular carcinoma appears as a small, solid nodule with spiculated borders.

Tubular Carcinoma Findings

- *On mammography*, tubular carcinoma often presents as a small spiculated mass, associated with suspicious calcifications in half of cases. Frequently, it manifests as a small architectural distortion, increasing the diagnostic challenge with sclerosing adenosis and radial scar.
- *On US*, tubular carcinoma typically mimics IDC NOS (not otherwise specified), manifesting as a hypoechoic solid mass with ill-defined margins and posterior acoustic shadowing.
- *On MRI*, it presents as a mass with the typical kinetics of a malignant lesion.
- *On CEDM*, in our series, tubular carcinomas accounted for 6% of breast cancers; the kinetics pattern was characterized by a progressive enhancement in 69% of cases and by wash-out in 31% of cases. The morphology of enhancement presented as a mass in 92% of cases and as NME in 8% of cases (Figs. 13.15 and 13.16).

13.3.4 Invasive Lobular Carcinoma

Invasive lobular carcinoma (ILC) is the second most common histologic type of breast cancer, accounting for 10–15% of all invasive breast neoplasms [48]. Although ILC is associated with a higher rate of multiplicity and bilaterality (approximately 30%) than invasive ductal cancers at diagnosis, the overall survival rate for patients with ILC is slightly higher than that for patients with the usual types of invasive ductal carcinomas.

Mammographically, ILC is very difficult to diagnose because of its high rate of false negative results (up to 19%), with a sensitivity ranging from 57 to 81%; a possible explanation for this behaviour can be found in its histological features: in fact, tumour cells have the tendency to infiltrate the stroma in a single-file arrangement without formation of a mass or development of associated fibrosis [49, 50]. Malignant cells may surround acini or ducts, creating a characteristic "bull's-eye" pattern. The diffuse spread of neoplastic cells in ILC is also reflected by its unusual metastatic pattern: ILC is far more likely to metastasize to the peritoneum-retroperitoneum, gastrointestinal tract, urogenital tract, leptomeninges and myocardium with respect to IDC. Histological variants of ILC include signet ring, alveolar, solid and pleomorphic types.

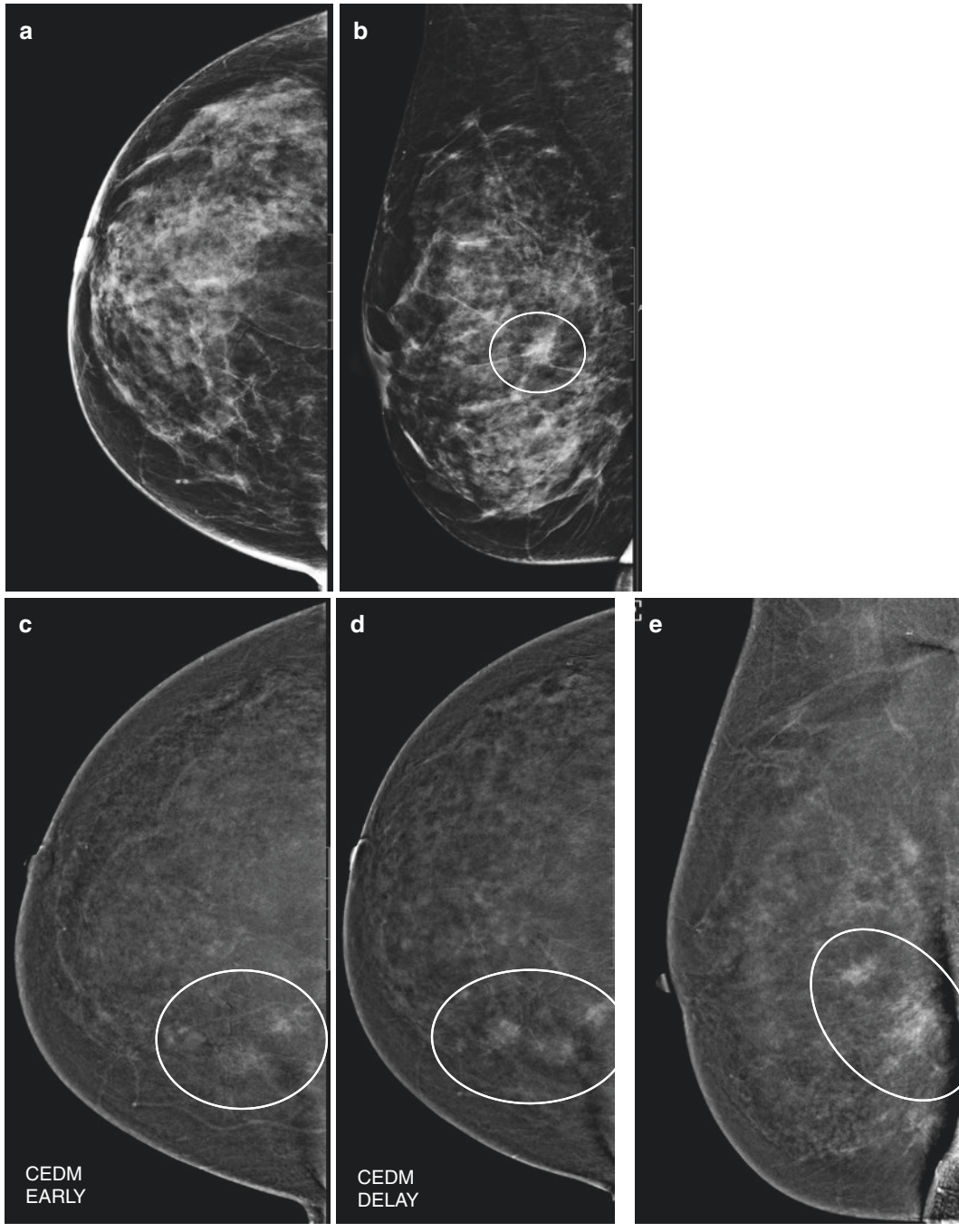

Fig. 13.14 Pre-surgical staging in a patient with a palpable BI-RADS 6 lesion in the central quadrants of the right breast. (**a**, **b**) Low energy 2D images in CC and MLO projections show a deep-seated suspicious mass with spiculated borders in the central-outer quadrant (*circle*). (**c**, **d**) CEDM recombined image in the early and late phase in CC projection. (**e**) CEDM recombined image in MLO projection. The examination shows the known lesion as an area of non-mass enhancement in the lower-inner quadrant (*circle*), demonstrating progressive enhancement kinetics. *Diagnosis: The pathology was an infiltrative lobular carcinoma*

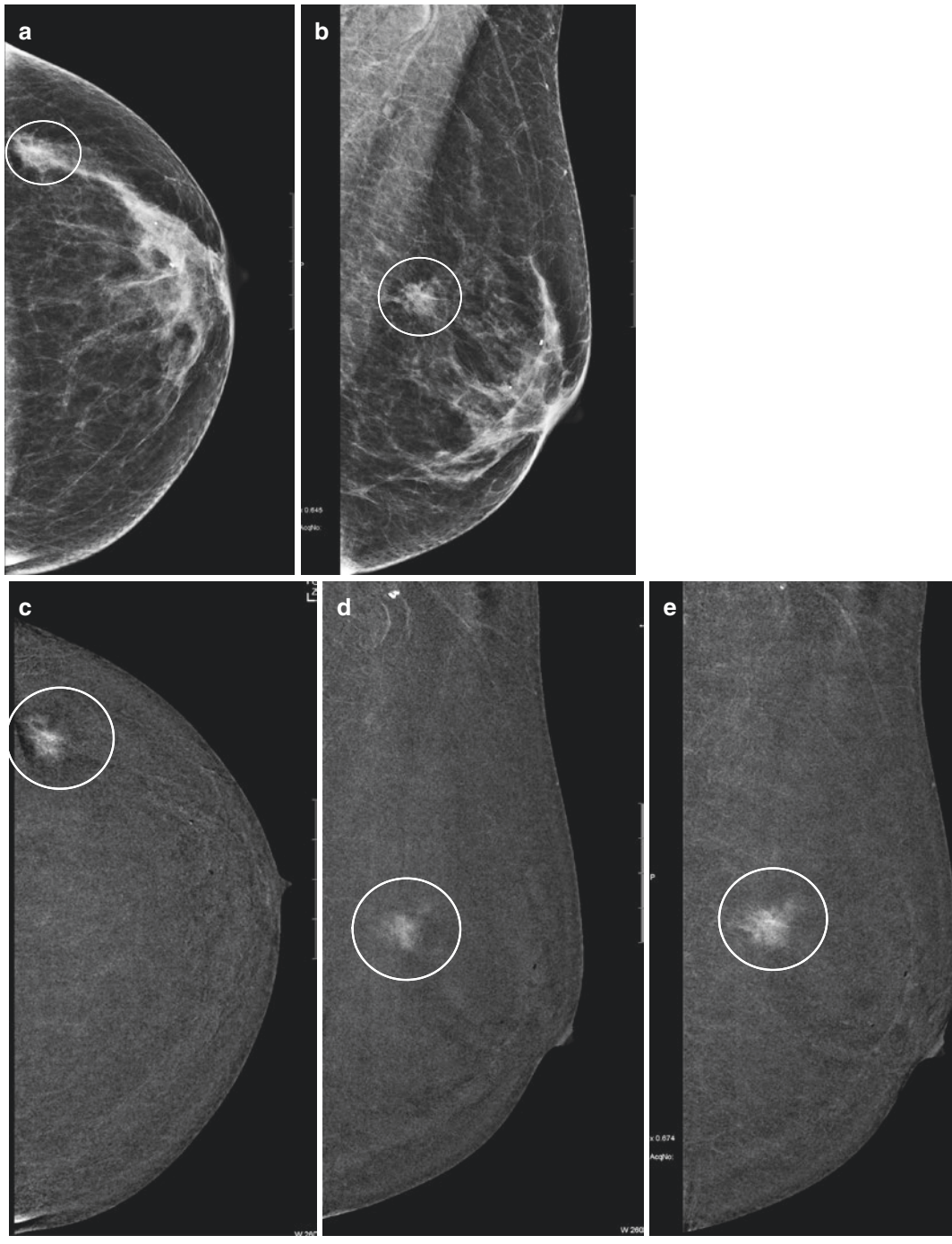

Fig. 13.15 Pre-surgical staging in a patient with a palpable BI-RADS 6 lesion in the central-outer quadrant of the left breast. (**a**, **b**) Low energy 2D images in CC and MLO projections show a deep-seated suspicious mass with spiculated borders in the central-outer quadrant (*circle*). (**c**) CEDM recombined image in CC projection. (**d**, **e**) CEDM recombined image in the early and late phase in MLO projection. The examination demonstrates the known mass as an intensely enhancing lesion with spiculated borders, showing progressive enhancement kinetics. *Diagnosis: The pathology was an infiltrative lobular carcinoma*

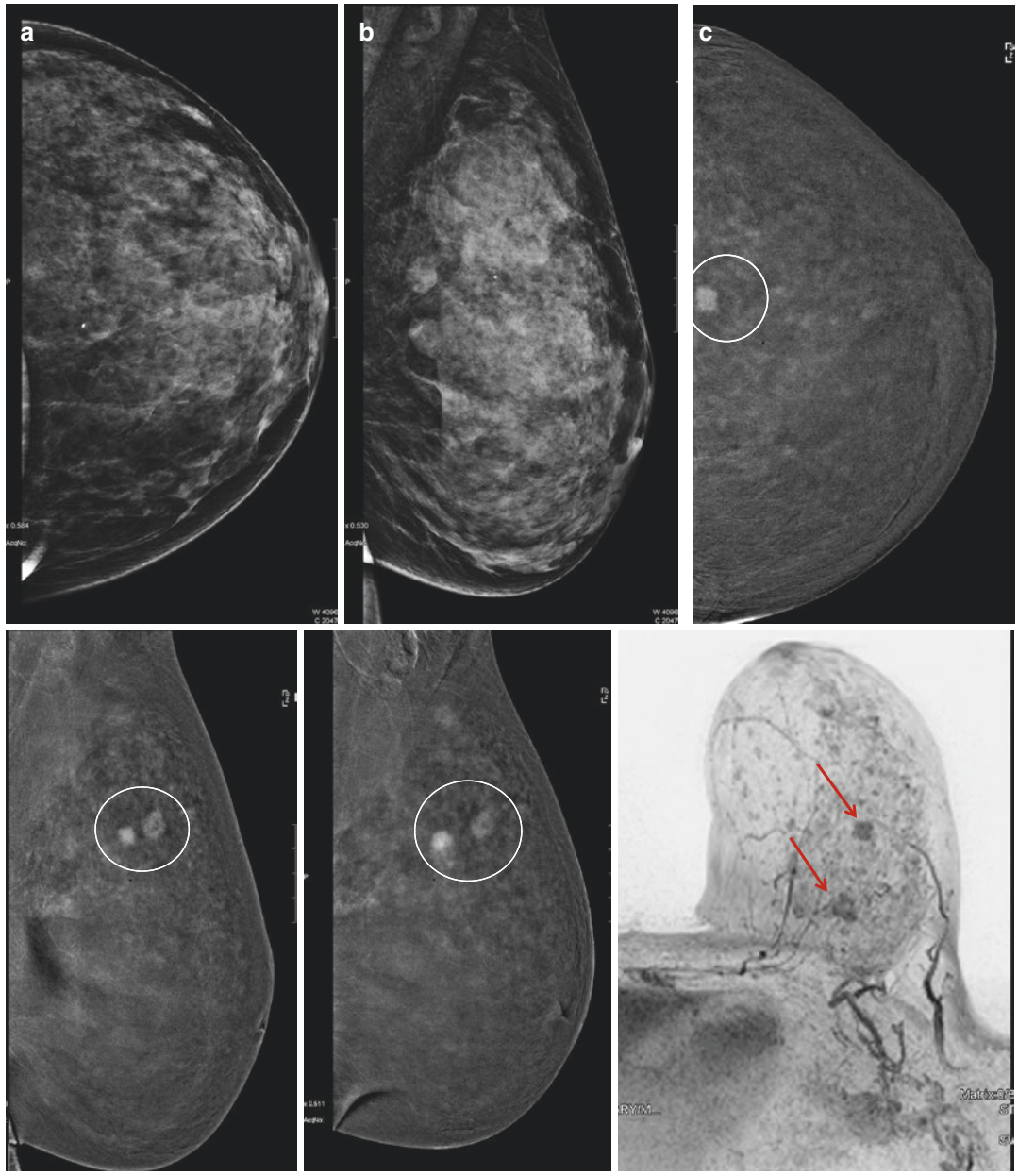

Fig. 13.16 Pre-surgical staging in a patient with a BI-RADS 6 lesion in the upper-outer quadrant of the left breast. (**a**, **b**) Low energy 2D images in CC and MLO projections show a relatively dense breast parenchyma. (**c**) CEDM recombined image in CC projection. (**d**, **e**) CEDM recombined image in the early and late phase in MLO projection. The examination demonstrates two intensely enhancing masses in the upper outer quadrant. However, the second lesion is not visualised on the CC view in view of the deep-seated location, which is among the limitations of CEDM. These lesions are seen to demonstrate a progressive enhancement. (**f**) MIP reconstruction on axial plane depicts both the lesions (*red arrows*) well, including the posteriorly located lesion, which was not seen on the CC view of the recombined images. *Diagnosis: The pathology was an infiltrative lobular carcinoma*

13.3.4.1 Invasive Lobular Carcinoma Findings

- *On mammography*, ILC commonly manifests as an opacity (44–65% of cases), usually with spiculated or ill-defined margins. Round masses account for only 1–3% of cases. Architectural distortion and subtly increased asymmetric density are the other forms of appearance, with a reported incidence of 10–34% and 1–14%, respectively [50]. For its peculiar presentation, ILC's diagnosis may be very difficult, presenting often completely negative mammography.
- *On US*, the detection rate of ILC rises dramatically, ranging from 68 to 98% [51]; in fact, it has been proven that US is superior to mammography for identifying multicentricity and multifocality and more accurately reflects the size of a mass than does mammography or clinical examination. US may show a mass with hypoechoic and heterogeneous internal echoes, and posterior acoustic shadowing in an area of clinically palpable mass or mammographic asymmetric density or abnormality. More specifically, classic ILC tends to manifest as focal shadowing without a significant mass, whereas the pleomorphic type typically manifests as a shadowing mass. Signet ring, alveolar and solid subtypes are more likely to manifest as a lobulated, well-circumscribed mass [51–53].
- *On MRI,* the morphologic and kinetic appearance of ILC is variable, reflecting its histological features. To date, MRI has been shown to be superior to mammography and US in detecting multifocality and multicentricity and is the most reliable technique in estimating tumour size [54]. The most common manifestation of ILC on MRI is a focal enhancing mass with spiculated or ill-defined margins (31–43% of cases). Additional manifestations include a dominant lesion surrounded by multiple small enhancing foci, multiple small enhancing foci with interconnecting enhancing strands, architectural distortions, diffuse enhancement patterns resembling normal glandular patterns and normal findings [54, 55]. A typical dynamic feature of ILC is the tendency to demonstrate a delayed progressive enhancement, with wash-out exhibited by only a minority of lesions.
- *On CEDM*, the MRI kinetics are similar to those observed in CEDM, in our experience; ILC, which accounted for 12% of all tumours, presented a delayed enhancement in 72% of cases, whereas only 28% of ILCs showed wash-out. An irregular mass was observed in 83% of cases and NME in 17% of cases. A possible explanation of this behaviour may rely on the histologic tendency of ILC to spread diffusely through the breast stroma in a lipid-filled pattern without exhibiting a nodular mass; thus, the enhancing portion may correspond to the normal parenchyma, which manifests as progressive enhancement.

Nevertheless, these data need further confirmation. In 28% of cases, CEDM detected an unsuspected cancer in the contralateral breast, proving the importance of functional imaging in staging multicentric/multifocal tumour: of these five new lesions, four were ILCs, and one was a lobular intraepithelial neoplasia (LIN1) (Figs. 13.17, 13.18, and 13.19).

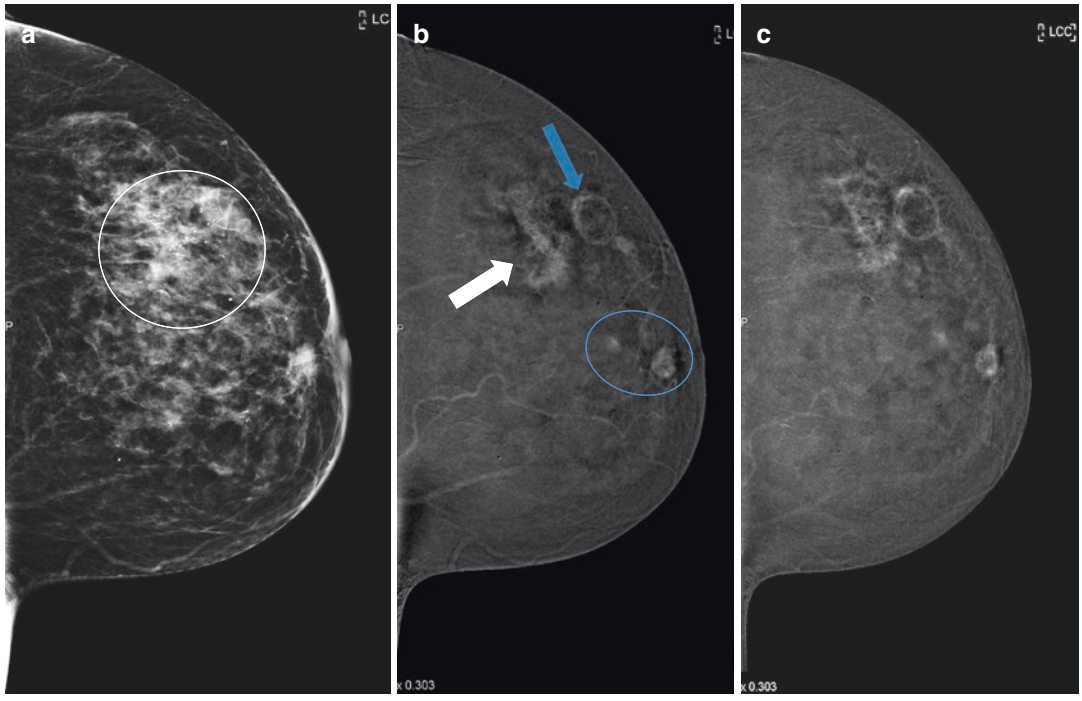

Fig. 13.17 Pre-surgical staging in a patient with a BI-RADS 6 lesion in the upper-outer quadrant of the left breast. (**a**) Low-energy 2D images in the CC projection show a cluster of heterogeneous calcifications with a regional distribution (*white circle*). (**b**, **c**) CEDM recombined image in the early and late phase in the CC projection. The examination shows a rim-enhancing lesion at the site of previous biopsy (*blue arrow*) in keeping with a post-biopsy haematoma. There is an associated area of non-mass enhancement seen posterior to it (*white arrow*), and there are two retroareolar masses which demonstrate wash-out in late images (*blue circle*). *Diagnosis: The pathology was ductal carcinoma in situ*

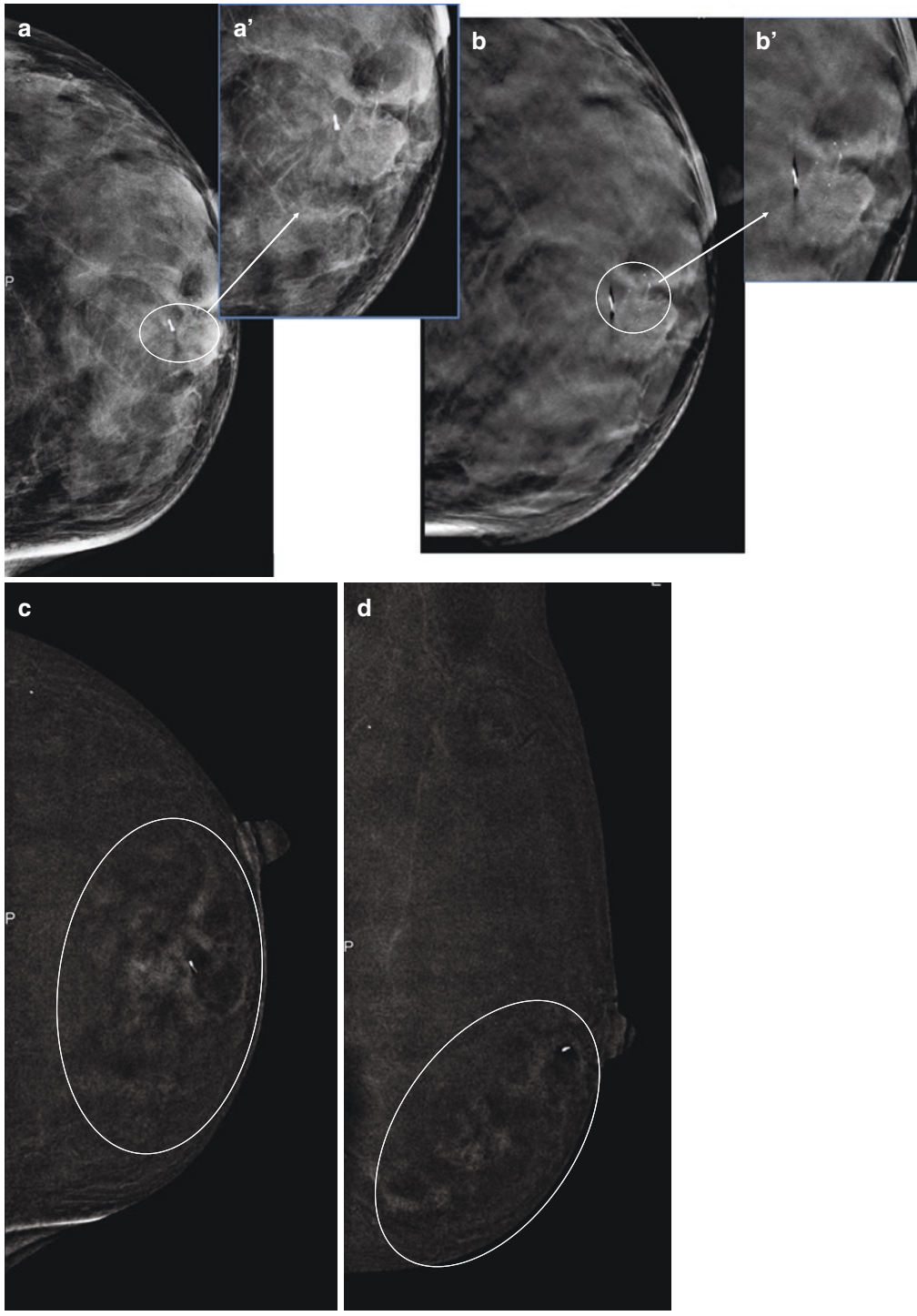

Fig. 13.18 Pre-surgical staging in a patient with a BI-RADS 6 lesion in the lower-inner quadrant of the left breast, already biopsied. (**a**, **a′**) Low-energy 2D images in the CC projection demonstrating a very dense breast with a suspicious cluster of fine pleomorphic cluster of calcifications (*circle*). (**b**, **b′**) 3D in CC projection depicts the calcifications and its distribution better (*circle*). (**c**, **d**) CEDM recombined image in the CC and MLO projections demonstrates an area of non-mass enhancement with regional distribution in the lower-inner and central-inner quadrants. The area of enhancement was much larger than the focal distribution of calcifications seen on the non-contrasted images. *Diagnosis: The pathology was a multicentric invasive ductal carcinoma*

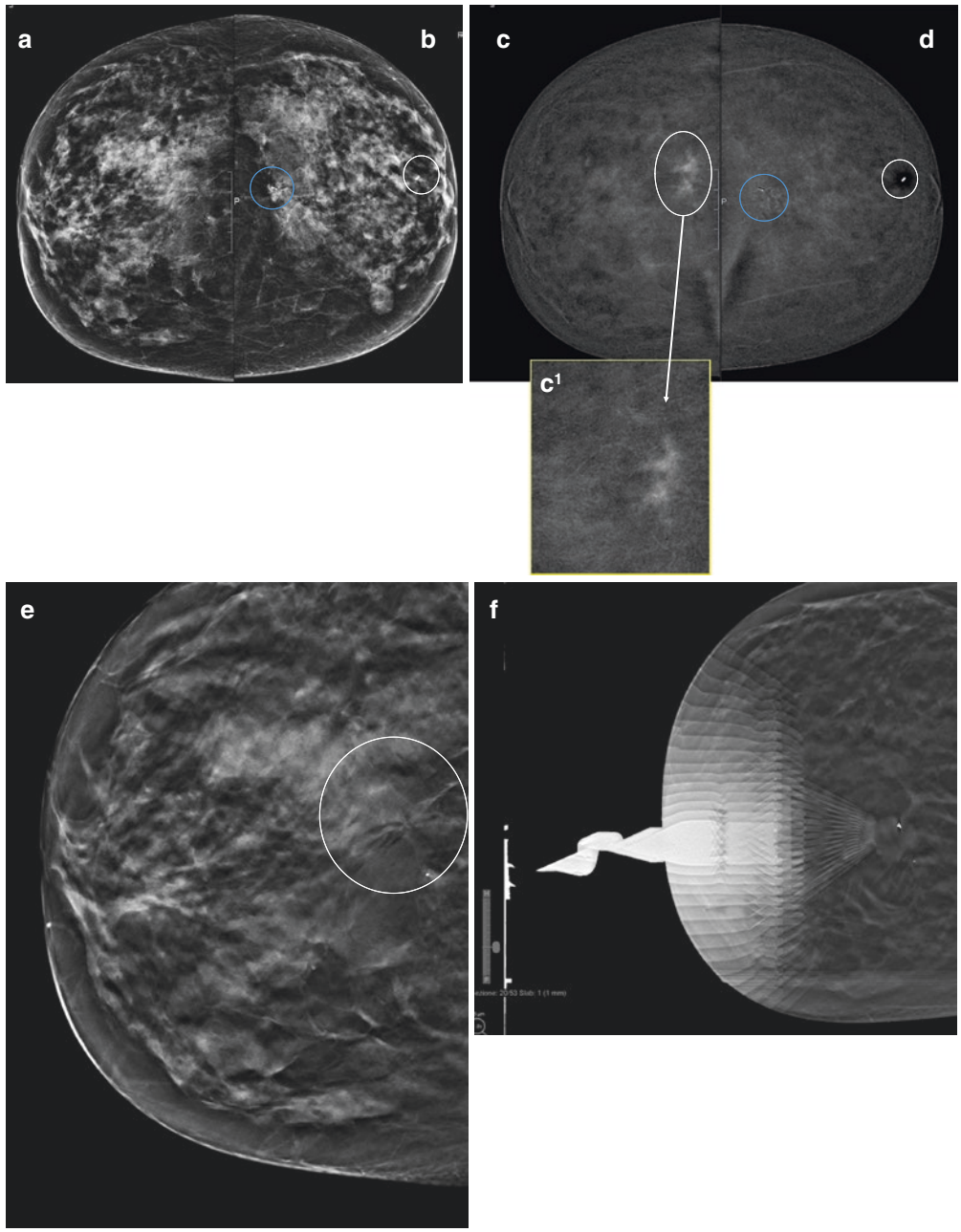

Fig. 13.19 A problem-solving case in a woman with dense breast and discordances between mammogram findings and histology results. (**a**, **b**) 2D FFDM low-energy 2D images in the CC projection show the two post-biopsy clips (*circles*), one at the lower-central quadrant and one at the superior-central quadrant both of the left breast. No obvious abnormalities are evident in the right breast. The histologic result of the two biopsy sites was B2, benign lesions, but the radiologic appearances of the architectural distortion were highly suggestive for malignancy. (**c**, **d**) CEDM recombined image in the early phase in CC projection shows a mild enhancement of the lesion in the posteriorly biopsied site (*blue circle*) of the left breast. (**c**, **c**[1]) However, there was an intense non-mass enhancement seen in the right breast in the central quadrant, which is better depicted in the magnified image. (**e**, **f**) 3D images were retrospectively reviewed after the CEDM exam, which showed an area of distortion corresponding to the enhancing site on recombined images. We later performed a tomosynthesis-guided stereotactic biopsy on the right breast. *Diagnosis: The pathology of the right lesion was a 10 mm multifocal ductal carcinoma in situ (DCIS), while the left breast lesion (blue circle) was a 4.5 mm infiltrating carcinoma*

References

1. Siegel RL, Miller KD, Jemal A. Cancer statistics, 2017. CA Cancer J Clin. 2017;65:5–29.
2. Folkman J. Role of angiogenesis in tumor growth and metastasis. Semin Oncol. 2002;29(6 Suppl 16):15–8.
3. Folkman J. New perspectives in clinical oncology from angiogenesis research. Eur J Cancer. 1996;32A:2534–9.
4. Gasparini C, Harris A. Clinical importance of the determination of tumor angiogenesis in breast carcinoma: much more than a new prognostic tool: review. J Clin Oncol. 1995;13:765–82.
5. Chu JS, Lee WJ, Chang TC, Chang KJ, Hsu HC. Correlation between tumor angiogenesis and metastasis in breast cancer. J Formos Med Assoc. 1995;94:373–8.
6. Barrett T, Brechbiel M, Bernardo M, Choyke PL. MRI of tumor angiogenesis. J Magn Reson Imaging. 2007;26:235–49.
7. Jong RA, Yaffe MJ, Skarpathiotakis M, et al. Contrast-enhanced digital mammography: initial clinical experience. Radiology. 2003;228(3):842–50.
8. Lewin JM, Isaacs PK, Vance V, Larke FJ. Dual-energy contrast-enhanced digital subtraction mammography: feasibility. Radiology. 2003;229(1):261–8.
9. Dromain C, Balleyguier C, Adler G, Garbay JR, Delaloge S. Contrast-enhanced digital mammography. Eur J Radiol. 2009;69(1):34–42.
10. Diekmann F, Freyer M, Diekmann S, et al. Evaluation of contrast-enhanced digital mammography. Eur J Radiol. 2011;78(1):112–21.
11. Jochelson M. Contrast-enhanced digital mammography. Radiol Clin North Am. 2014;52(3):609–16.
12. Diekmann F, Marx C, Jong R, Dromain C, Toledano AY, Bick U. Diagnostic accuracy of contrast enhanced digital mammography as an adjunct to mammography. Eur Radiol. 2007;17(12):3086–92.
13. Dromain C, Thibault F, Muller S, et al. Dual-energy contrast-enhanced digital mammography: initial clinical results. Eur J Radiol. 2011;21:565–74.
14. Jochelson MS, Dershaw DD, Sung JS, et al. Bilateral contrast-enhanced dual-energy digital mammography: feasibility and comparison with conventional digital mammography and MR imaging in women with known breast carcinoma. Radiology. 2013;266:743–51.
15. Sogani J, Morris EA, Kaplan JB, et al. Comparison of background parenchymal enhancement at contrast-enhanced spectral mammography and breast MR imaging. Radiology. 2017;282(1):63–73. https://doi.org/10.1148/radiol.2016160284.
16. Bhimani C, Matta D, G Roth R, et al. Contrast enhanced spectral mammography: techniques, indications and clinical applications. Acad Radiol. 2017;24:84–8.
17. Lalji U, Lobbes M. Contrast-enhanced dual-energy mammography: a promising new imaging tool in breast cancer detection. Womens Health. 2014;10(3):289–98.
18. Lobbes MB, Smidt ML, Houwers J, et al. Contrast-enhanced mammography: techniques, current results, and potential indications. Clin Radiol. 2013;68:935–44.
19. Hobbs MM, Taylor DB, Buzynski S, Peake RE. Contrast-enhanced spectral mammography (CESM) and contrast enhanced MRI (CEMRI): patient preferences and tolerance. J Med Imaging Radiat Oncol. 2015;59(3):300–5.
20. Silverstein MJ, Poller DN, Waisman JR, et al. Prognostic classification of breast ductal carcinoma-in-situ. Lancet. 1995;345(8958):1154–7.
21. Lagios MD. Heterogeneity of duct carcinoma in situ (DCIS): relationship of grade and subtype analysis to local recurrence and risk of invasive transformation. Cancer Lett. 1995;90(1):97–102.
22. Dershaw DD, Abramson A, Kinne DW. Ductal carcinoma in situ: mammographic findings and clinical implications. Radiology. 1989;170(2):411–5.
23. Holland R, Hendriks JH, Vebeek AL, Mravunac M, Schuurmans Stekhoven JH. Extent, distribution, and mammographic/histological correlations of breast ductal carcinoma in situ. Lancet. 1990;335(8688):519–22.
24. Yang WT, Tse GMK. Sonographic, mammographic, and histopathologic correlation of symptomatic ductal carcinoma in situ. AJR Am J Roentgenol. 2004;182(1):101–10.
25. Douglas-Jones AG, Morgan JM, Appleton MA, et al. Consistency in the observation of features used to classify duct carcinoma in situ (DCIS) of the breast. J Clin Pathol. 2000;53(8):596–602.
26. Consensus Conference Committee. Consensus conference on the classification of ductal carcinoma in situ. Cancer. 1997;80(9):1798–802.
27. Lee KS, Han BH, Chun YK, Kim HS, Kim EE. Correlation between mammographic manifestations and averaged histopathologic nuclear grade using prognosis-predict scoring system for the prognosis of ductal carcinoma in situ. Clin Imaging. 1999;23(6):339–46.
28. Berg WA, Gutierrez L, NessAiver MS, et al. Diagnostic accuracy of mammography, clinical examination, US, and MR imaging in preoperative assessment of breast cancer. Radiology. 2004;233(3):830–49.
29. Orel SG, Mendonca MH, Reynolds C, Schnall MD, Solin LJ, Sullivan DC. MR imaging of ductal carcinoma in situ. Radiology. 1997;202(2):413–20.
30. Mokbel K. Current management of ductal carcinoma in situ of the breast. Int J Clin Oncol. 2003;8(1):18–22.
31. Kuhl CK, Schrading S, Bieling B, et al. MRI for diagnosis of pure ductal carcinoma in situ: a prospective observational study. Lancet. 2007;370:485–92.
32. Yamada T, Mori N, Watanabe M, et al. Radiologic-pathologic correlation of ductal carcinoma in situ. Radiographics. 2010;30(5):1183–98.

33. Tozaki M, Igarashi T, Fukuda K. Breast MRI using the VIBE sequence: clustered ring enhancement in the differential diagnosis of lesions showing non-mass like enhancement. AJR Am J Roentgenol. 2006;187(2):313–21.
34. Morakkabati-Spitz N, Leutner C, Schild H, Traeber F, Kuhl C. Diagnostic usefulness of segmental and linear enhancement in dynamic breast MRI. Eur Radiol. 2005;15(9):2010–7.
35. Mossa-Basha M, Fundaro GM, Shah BA, Ali S, Pantelic MV. Ductal carcinoma in situ of the breast: MR imaging findings with histopathologic correlation. Radiographics. 2010;30(6):1673–87.
36. Heywang-Köbrunner SH. Contrast-enhanced magnetic resonance imaging of the breast. Invest Radiol. 1994;29(1):94–104.
37. Cheung YC, Juan YH, Lin YC, et al. Dual-Energy Contrast enhanced spectral mammography: enhancement analysis on BI-RADS 4 non mass microcalcifications in screened women. PLoSOne. 2016;11(9):e0162740. https://doi.org/10.1371/journal.pone.0162740.
38. Luczynska E, Niemiec J, Hendrick E, et al. Degree of enhancement on contrast enhanced spectral mammography (CESM) and lesion type on mammography (MG): comparison based on histological results. Med Sci Monit. 2016 Oct 21;22:3886–93.
39. Fallenberg E, Dromain C, Diekmann F, et al. Contrast-enhanced spectral mammography versus MRI: initial results in the detection of breast cancer and assessment of tumour size. Eur J Radiol. 2014;24:256–64.
40. Carriero A, Ambrossini R, Mattei PA, et al. Magnetic resonance of the breast: correlation between enhancement patterns and microvessel density in malignant tumors. J Exp Clin Cancer Res. 2002;21(Suppl 3):83–7.
41. Yamaguchi R, Furusawa H, Nakahara H, et al. Clinicopathological study of invasive ductal carcinoma with large central acellular zone: special reference to magnetic resonance imaging findings. Pathol Int. 2008;58(1):26–30.
42. World Health Organization. Histological typing of breast tumors. Tumori. 1982;68:181–98.
43. Okafuji T, Yabuuchi H, Sakai S, et al. MR imaging features of pure mucinous carcinoma of the breast. Eur J Radiol. 2006;60(3):405–13.
44. Kawashima M, Tamaki Y, Nonaka T, et al. MR imaging of mucinous carcinoma of the breast. AJR Am J Roentgenol. 2002;179(1):179–83.
45. Soo MS, Williford ME, Walsh R, Bentley RC, Kornguth PJ. Papillary carcinoma of the breast: imaging findings. AJR Am J Roentgenol. 1995;164(2):321–6.
46. Lam WW, Tang AP, Tse G, Chu WC. Radiology-pathology conference: papillary carcinoma of the breast. Clin Imaging. 2005;29(6):396–400.
47. Kuhl CK, Klaschik S, Mielcarek P, Gieseke J, Wardelmann E, Schild HH. Do T2-weighted pulse sequences help with the differential diagnosis of enhancing lesions in dynamic breast MRI? J Magn Reson Imaging. 1999;9(2):187–96.
48. Arpino G, Bardou VJ, Clark GM, Elledge RM. Infiltrating lobular carcinoma of the breast: tumor characteristics and clinical outcome. Breast Cancer Res. 2004;6(3):R149–56.
49. Dixon JM, Anderson TJ, Page DL, Lee D, Duffy SW, Stewart HJ. Infiltrating lobular carcinoma of the breast: an evaluation of the incidence and consequence of bilateral disease. Br J Surg. 1983;70(9):513–6.
50. Lopez JK, Bassett LW. Invasive lobular carcinoma of the breast: spectrum of mamographic, US, and MR imaging findings. Radiographics. 2009;29:165–76.
51. Paramagul CP, Helvie MA, Adler DD. Invasive lobular carcinoma: sonographic appearance and role of sonography in improving diagnostic sensitivity. Radiology. 1995;195(1):231–4.
52. Butler RS, Venta LA, Wiley EL, Ellis RL, Dempsey PJ, Rubin E. Sonographic evaluation of infiltrating lobular carcinoma. AJR Am J Roentgenol. 1999;172(2):325–30.
53. Selinko VL, Middleton LP, Dempsey PJ. Role of sonography in diagnosing and staging invasive lobular carcinoma. J Clin Ultrasound. 2004;32(7):323–32.
54. Mann RM, Hoogeveen YL, Blickman JG, Boetes C. MRI compared to conventional diagnostic work-up in the detection and evaluation of invasive lobular carcinoma of the breast: a review of existing literature. Breast Cancer Res Treat. 2008;107(1):1–14.
55. Weinstein SP, Orel SG, Heller R, et al. MR imaging of the breast in patients with invasive lobular carcinoma. AJR Am J Roentgenol. 2001;176(2):399–406.